M I S T

ANNA L. GOENSE - JULY 2018

MIST ⊢⟶ IN PARTIAL FULLFILMENT OF THE REQUIREMENTS FOR THE **DEGREE OF** *MASTER OF SCIENCE* **IN** *CIVIL ENGINEERING***.**

BY *ANNA L. GOENSE*

THESIS COMMITTEE:
PROF. DR. IR. NICK VAN DE GIESEN
DR. IR. ROLF HUT
DR. IR. BAS HEIJMAN

TO BE DEFENDED PUBLICLY ON
23 JULY 2018

T́U Delft

IK HEB HET NOG NOOIT GEDAAN, DUS IK DENK DAT IK HET WEL KAN

- Pippi Langkous

Before anything else

This document is made as part of a thesis project of the master Water Management at the Faculty of Civil Engineering at the Delft University of Technology. During this project, we found that the current analytical design model for fog water catchers does not apply to all fog water catcher shapes. After the introduction, in the second chapter, you will find a paper in the academic style elaborating further on this topic with the title: "Fog Water Collection Efficiency: The Influence of Collector Geometry." Later in this document often referred to as "the paper."

The remainder aims to inspire other students, researchers, NGOs, designers, or anybody interested, to use the findings of this project to develop better fog harvesters in the future. There is a focus on methodology, and I have made the conscious choice to write in an accessible manner.

The third chapter elaborates further on the computational fluid dynamics model that was used during this study. The last three chapters focus on the experimental methods that have been used during this research project. Starting with the construction of the climatic wind tunnel, followed by an overview of all prototype fog catchers that have been tested, and concluding with all experimental results.

Acknowledgements

I am grateful to everyone that has supported me during this project. First of all, I would like to thank the members of my thesis committee, Bas Heijman, Nick van de Giesen, and in particular Rolf Hut. As my daily supervisor, you have helped me tremendously throughout my thesis, encouraging me with your enthusiasm, creativity, and sharp mind. Most of all you taught me how to get research done, a valuable lesson on when I should stop thinking, and start doing.

The spark of inspiration for this research came from the Moroccan NGO, Dar Si Hmad. I would like to thank them for the initial visit to their office last summer that started my enthusiasm for fog harvesting. Abbes Benaissa especially, who was always willing to answer my questions about fog harvesting throughout this project.
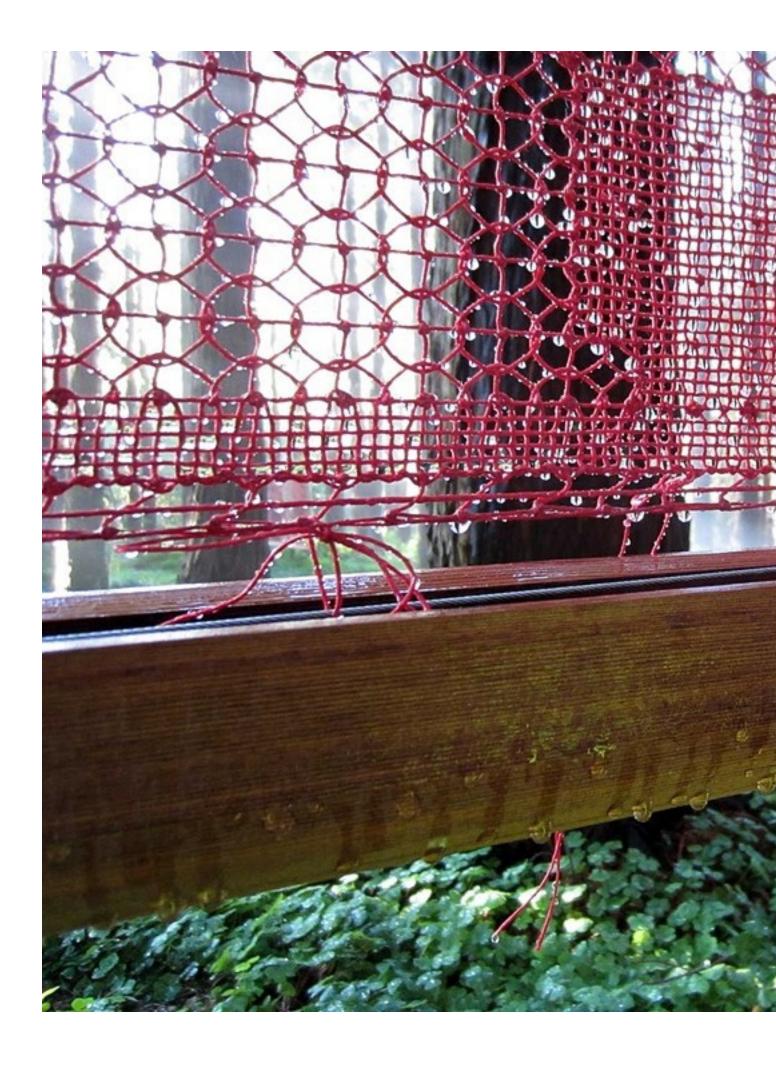
Without the people at the Stevin II lab of the faculty of civil engineering, this research would not have been possible. I would like to thank Mohammed Jafar for guiding me, and Ton Blom for helping me out with whatever I needed inside the climate room, however strange the request.

My written work has improved tremendously because of careful review by others. Thank you, Lucia, James, and Niek for your critical eyes and perfectionism, and Rolf for teaching me how to write an academic article. Those red pages were always a gift.

Aside from the contributions mentioned above, I would not have been able to accomplish this project without the unconditional love and support of my father, brothers, and sister. My roommates, who were always there in the kitchen to offer a sympathetic ear. Yoga teacher René, who helped me remember that I have a body that needs nurturing too. And the positive energy from all students that have passed through room 4.84.

Thank you, Odilia and James, for keeping me sane during the last two days.

Anna L. Goense
Delft, 16 July 2018

INDEX

THE Craft OF Research

WAYNE

GREGOR

JOSEPH

Prologue

BECOMING A RESEARCHER

WHO NEEDS RESEARCH?

When you think of a researcher, what do you imagine? Someone in a lab coat peering into a microscope? A white-bearded professor taking notes in a silent library? That's what most people think. But you might also have pictured Oprah, Yahoo creator Jerry Yang, or the manager of every major league baseball, football, and basketball team in the world. Like just about every successful person, they are not only experts in doing research, but in using the research of others. In fact, that's part of what makes them successful. In an aptly named "age of information" (or, too often, *mis*-information), every one of them has learned not only how to find information, but how to evaluate it, then to report it clearly and accurately. More than ever, those skills are essential to anyone who wants to succeed in just about any profession you can think of.

You may not yet be one of those practicing professionals, but learning to do research now will help you today and prepare you for what's to come. First, it will help you understand what you read as nothing else will. You can accurately judge the research of others only after you've done your own and can understand the messy reality behind what is so smoothly and confidently presented in your textbooks or by experts on TV. The Internet and cable TV flood us with "facts" about government, the economy, the environment, the products we buy. Some are sound; most are not. That's why, as you

1. Introduction

The World Health Organization (WHO) estimates there are 844 million people who lack basic drinking water services.[1] This means that either water collection times exceed 30 minutes, water is taken from an unimproved source, or people live under the double burden of both. Every day, millions of girls spend hours of their day getting water for their family, time that could have been spent going to school. The exploration of unconventional water resources that have not yet been utilized, such as the water in the air, is necessary to meet (future) water demands.

Fog harvesting is a low cost, low tech, drinking water solution for arid regions where fog occurs on a regular basis. Capturing fog doesn't have to be anything fancy. Build a simple frame, hang the right net in there, and a community with the right climatic circumstances can start capturing fog from the air.

The power of fog harvesting is its simplicity.

The technology also appeals to the imagination of researchers and designers. Biomimetic and innovative designs have been researched and developed, focusing on improving the impaction and draining efficiency by inventing new mesh materials.

Earlier studies on the aerodynamics of fog catchers have suggested that the efficiency of fog catchers can be improved by changing the shape of the catcher while keeping the material cheap and accessible.[2,3] Therefore, I started this project to create a better understanding of how the geometry of fog catchers influences the water collection efficiency. We discovered that building fog water catchers convexly facing the wind can collect more fog water than previously expected.

The results of this project can be used as a starting point to design a reliable and economically feasible fog harvester with high efficiency. CFD simulations and prototype testing in a small-scale wind tunnel could be used as design tools. The following chapter will present a consisely written paper attending to the most important findings. The remainder of this document aims to give an accessible overview of the methods used during this project and present results that cannot be given justice to in the paper but contain relevant lessons for anyone picking up this research.

[1]UNICEF, & WHO. (2017). Progress on Drinking Water, Sanitation and Hygiene. https://doi.org/10.1111 / tmi.12329
[2] Rivera, J. D. D. (2011). Aerodynamic collection efficiency of fog water collectors. Atmospheric Research, 102(3), 335–342. https://doi.org/10.1016/j.atmosres.2011.08.005
[3] Holmes, R., De Dios, J., & De La Jara, E. A. (2015). Large fog collectors: New strategies for collection efficiency and structural response to wind pressure. Atmospheric Research, 151, 236–249. https://doi.org/10.1016/j.atmosres.2014.06.005

2. Fog Water Collection Efficiency: The Influence of Collector Geometry

A. L. Goense

Department of Water Management, Delft University of Technology

R. W. Hut

Department of Water Management, Delft University of Technology

S. G. J. Heijman

Department of Water Management, Delft University of Technology

1 Abstract

Fog harvesting is a sustainable drinking water solution for arid climates. Previous studies have developed an analytical model to predict the fog water collection efficiency as a product of aerodynamic and deposition efficiency as independent factors. In this study, we tested the assumption that deposition efficiency stays unchanged when the geometry of the fog catcher is adjusted. We assessed the collection efficiency of both straight and curved fog water collectors using computational fluid dynamics models and performed controlled experiments in a climatic wind tunnel on sample fog water collectors. The analytical model disregards convex fog harvesters because their lower drag coefficient reduces the aerodynamic efficiency of the fog harvester. The results of the CFD models show that efficiency can be doubled if fog catchers are built convex facing the wind. The wind tunnel experiments support the results from the CFD models. The results of this study show that for convex fog harvesters, although less fog passes through the net, the deposition efficiency increases resulting in a net increase of water collection.

2   Fog Water Collection Efficiency: The Influence of Collector Geometry

3   Introduction

Fog harvesting is a low cost, low tech, drinking water solution for arid and semi-arid regions where fog occurs on a regular basis. Several operating projects have already successfully shown that fog harvesting is a sustainable solution for providing drinking and irrigation water (Batisha, 2015; Klemm et al., 2012; Wahab, Lea, Abdul-wahab, & Lea, 2008). The quality of fog water is within the safety range specified by the WHO (Schunk et al., 2018; Schemenauer & Cereceda, 1992), and the time needed to collect water by the users are often significantly lower when fog harvesters are installed (Klemm et al., 2012).

In practice, most fog water collectors (FWCs) consist of two poles or a rectangular frame, perpendicular to the dominant direction of the wind-driven fog, in which a mesh material is suspended. Biomimetic and innovative designs for fog harvesting have been researched and prototyped, predominantly focusing on developing new mesh materials to increase water collection (Azad, Ellerbrok, Barthlott, & Koch, 2015; White, Sarkar, & Kietzig, 2013; Ebner, Miranda, & Roth-nebelsick, 2011; Park, Chhatre, Srinivasan, Cohen, & McKinley, 2013). However, in the field, simple open fabric, such as greenhouse shade nets, is what is predominantly used for fog harvesting purposes (Regalado & Ritter, 2016).

Fog water collection rates vary dramatically from site to site, but yearly averages from 3 to 10 $^{L}/_{m^2day}$ are typical for operational projects (Klemm et al., 2012). The collection rate is determined by the wind speed, liquid water content, size distribution of fog droplets, and the type of FWC that is used (Batisha, 2015). The water collection efficiency of the FWC is defined as the fraction of water that is collected from the air. Schemenauer and Joe (1989) measured efficiencies of 20% for a large FWC in Chile using a simple Raschel mesh.

Current design practises estimate the efficiency of a FWC to be a product of the aerodynamic efficiency, deposition efficiency, and drainage efficiency ((Rivera, 2011; Park et al., 2013; Shi, Anderson, Tulko, Kennedy, & Boreyko, 2018; Regalado & Ritter,

2016, 2017). With the FWC positioned perpendicular to the dominant wind speed, the aerodynamic efficiency represents the fraction of water carrying air approaching the FWC that actually flows through the mesh, instead of around it. The deposition efficiency represents the fraction of droplets that subsequently collide with the mesh wires. As more droplets collide with the mesh, the impinged water coalesces and bigger droplets form. When droplets reach a critical volume they flow down along the mesh to be collected in a reservoir. However, droplets impacted on the wires can also stay attached, be deflected or spill, which is represented by the drainage efficiency.

In this study we analyse fog water collection efficiency of different FWCs using computational fluid dynamics (CFD) models. De la Jara (2012) and Holmes et al. (2015) previously used CFD models to analyse the feasibility of concave funnel-shaped fog harvesting devices. Where de la Jara (2012) and Holmes et al. (2015) focused on calculating the efficiency for specific designs, we test the assumption that aerodynamic and deposition efficiency are independent factors in the estimation of the total water collection efficiency. We assess the effect of geometry by looking at both straight and curved FWCs. To connect theory to practice, the CFD results are compared to experiments of sample FWCs in a climatic wind tunnel.

In this paper we first review the current analytical model for fog water collection efficiency in 4.1. Next we describe the setup of the CFD models and the experiments in section 4.2 and 4.3, respectively. Results are presented in section 5 and discussed in section 6.

4 Materials and methods

4.1 Analytical fog water collection efficiency

4.1.1 Aerodynamic efficiency. Rivera (2011) developed a simplified two-dimensional flow model to determine the aerodynamic efficiency of FWCs, i.e. the fraction of air that will pass through the mesh instead of around. The model proposes a superposition of a fog flow that passes around a solid screen and a flow forced to pass only through a mesh, Based on this approximation, the model is able to find the

balance between the drag force on the FWC and the pressure drop over the net. This results in an expression for the aerodynamic efficiency governed by three dimensionless parameters, as shown in equation (1).

$$\eta_a = \frac{S_c}{1 + \sqrt{C_o/C_d}} \tag{1}$$

S_c represents the shade coefficient (SC), which is the fraction of mesh area that is occluded by mesh wires; C_d is the drag coefficient of a non-permeable screen and is dependent on the shape of the screen; C_o is the pressure drop coefficient and depends on the SC, the type of wire, and knit of the mesh. Idel'chik (1960) published an overview of empirical formulas for C_o for different mesh types. Rivera (2011) and Park et al. (2013) propose to apply the basic correlation for a wire mesh: $C_o = 1.3 S_c + (\frac{S_c}{1-S_c})^2$ (Idel'chik, 1960), which we will use in this study.

For large enough Reynolds numbers, $(Re > 10^3)$, C_o and C_d are independent of the wind velocity (Regalado & Ritter, 2016; Rivera, 2011). Considering mesh dimensions of $4m \times 12m$ for an average sized FWC in the field and wind speeds $> 2\,m/s$ the Reynolds number is over $9.5 \cdot 10^5$. For smaller test collectors of one by one meter, the Reynolds number is over $1.4 \cdot 10^5$.

The model for aerodynamic efficiency suggests that when the fog catcher has a higher drag coefficient, the efficiency increases and there is an optimal SC after which efficiency declines again because the pressure drop over the net becomes larger.

4.1.2 Deposition efficiency. For the deposition efficiency, sometimes referred to as impaction collection efficiency in the literature, there are three possible aerosol deposition mechanisms: diffusion, interception, and inertial impaction. These all predominantly depend on the droplet size (Hahner, Dau, & Ebert, 1994). At fog harvesting sites droplet diameters of 2 to $30\,\mu m$ are found, with a high concentration peak around $10\,\mu m$ (Schemenauer & Joe, 1989). Diffusion occurs when smaller particles move due to Brownian motion and hit the surface of the mesh wires. However, this is only relevant for fog droplets with a diameter smaller than $0.1\,\mu m$ (Regan & Raynor, 2009). These droplets only make up a small fraction of the total liquid water content in

the fog, thus any water collected trough diffusion can be neglected (Schemenauer & Joe, 1989). During interception, particles following the air streamlines pass a mesh wire and get intercepted by the wire surface simply due to their size. For a mesh wire with a diameter of 1mm and with wind speed of 5 m/s, droplets with a diameter $> 100\,\mu m$ start to be intercepted (Regalado & Ritter, 2016). Since fog particles $> 18\,\mu m$ contribute little to the total liquid water content of the fog (Schemenauer & Joe, 1989) this deposition mechanism can also be neglected. The remaining deposition mechanism is inertial impaction. This occurs when particles cannot adjust to the sudden change of air streamlines around the mesh wire, and, due to their inertia, depart from the streamline and impact on the wire, see figure 1. Inertial impaction depends on the dimensionless Stokes number (S_{tk}) (Israel & Rosner, 1982), which is the ratio of the stopping distance of the droplet to the obstacle's characteristic length:
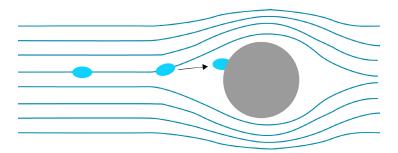
$$S_{tk} = \frac{\rho_w v_0 D_d^2}{18\mu_a D_w} \tag{2}$$

With ρ_w the density of water, v_0 the unperturbed wind velocity, D_d the droplet diameter, μ_a the dynamic viscosity of the air, and D_w the diameter of the net wire. Droplets with a low Stokes number will follow the fluid streamlines, whereas inertia dominates for droplets with a large Stokes number; these droplets will continue along their initial trajectory towards the mesh wire. Langmuir and Blodgett (1946) found that the inertial impaction efficiency can be described with an empirical formula solely dependent on the Stokes number, which we will use in this study:

$$\eta_d = \frac{S_{tk}}{S_{tk} + \pi/2} \tag{3}$$

Deposition efficiency steeply increases around $S_{tk} = 1$, up to a maximum where it reaches a plateau of 100%.

4.1.3 Drainage efficiency. After the droplets are deposited on a net wire, they coalesce until they reach a critical volume where the gravitational force overcomes the adhesion force and the larger droplet flows down along the wire to be collected in a reservoir. Drainage efficiency considers that some droplets will be lost due to

Figure 1. Droplet depostion on a single cylinder due to inertial impaction. When inertia dominates, droplets continue along their trajectory towards the cylinder and deposit.

entrainment in the air stream and spills, and that others can stay impinged on the mesh and clog the voids of the mesh, affecting the aerodynamic efficiency (Park et al., 2013). An extensive review of drainage efficiency and the interaction of mesh wettability, mesh knit, droplet diameter and wind speed is given in Park et al. (2013). Because this study focuses on the geometry of the FWC, we assume drainage efficiency is 1.

Summarizing, in this paper we consider the following analytical model for fog water collection efficiency:

$$
\begin{aligned}
\eta_c &= \eta_a \cdot \eta_d \\
\eta_c &= \frac{S_c}{1 + \sqrt{C_o/C_d}} \frac{S_{tk}}{S_{tk} + \pi/2} \\
\eta_c &= \frac{S_c}{1 + \sqrt{\frac{1.3 S_c + (\frac{S_c}{1 - S_c})^2}{C_d}}} \frac{\rho_w v_0 D_d^2}{\rho_w v_0 D_d^2 + 9 \mu_a D_w \pi}
\end{aligned}
\tag{4}
$$

4.2 Numerical fog water collection efficiency

We performed a set of numerical simulations to test the water collection efficiency for three scenarios. A single cylinder, straight nets with different SC, and nets with varying C_d. We chose these scenarios in order to analyse the influence of each variable of the analytical model. The main goal of the simulations is to check the analytical model, in particular the assumption that η_a and η_d are independent factors. All setup files of the simulation experiments are available as supplementary material.
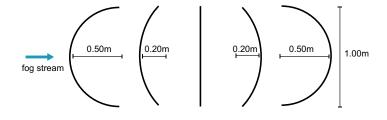
4.2.1 CFD modelling setup. We used the computational fluid dynamics (CFD) module Ansys FLUENT, version 18.2 to do the numerical simulations. The

Reynolds Average Navier Stokes (RANS) equations, coupled with a $k - \epsilon$ turbulence model, were solved for each scenario. We simulated the fog by coupling a discrete phase model (DPM) in which the trajectories of the droplets can be computed. All droplets impacting on the mesh were marked as collected.

4.2.2 Droplet deposition on a single cylinder. In order to study the effect of droplet size on the deposition efficiency, we modelled a single circle with a diameter of 1mm to represent one single net wire. By only modelling one circle, the deposition efficiency can be compared to the analytical model without the influence of losses due to the aerodynamic efficiency. Wind velocity was kept at a constant 4m/s, while we performed the simulation for six different droplet diameters. See table 1 for an overview.

4.2.3 Effect of SC on collection efficiency. We studied the effect of the shade coefficient on the collection efficiency of a straight FWC. The FWC was represented in the CFD analysis as a collection of equally spaced circles with a diameter of 1mm. The total frontal length of the FWC was kept at 1m, whereas the number of circles was adjusted in order to generate FWCs with different SCs. The SC is determined with: $S_c = \frac{n \cdot D_w}{L}$, with n the number of circles, D_w the circle diameter, and L the length of the FWC. In total we simulated 15 different SCs, see table 2.

4.2.4 Effect of FWC shape on collection efficiency. We analysed the effect of FWC shape on water collection efficiency by simulating five geometries with varying drag coefficients, see figure 2. Each geometry had an SC of 0.6 and was simulated for three different droplet diameters. We determined the drag coefficients for solid bodies of the same shape using Ansys FLUENT. An overview is given in table 3.
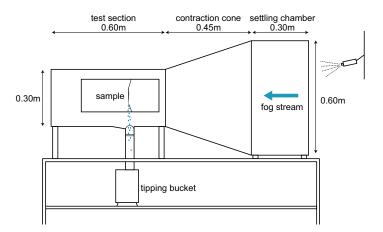

Figure 2. Schematic diagram of the five geometries with varying drag coefficient as tested in CFD model.
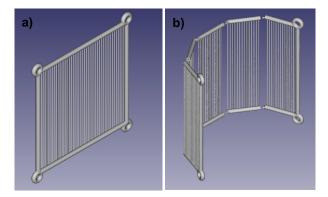
4.3   Experimental fog water collection

We performed a set of lab experiments to validate the water collection rates of the CFD models. We tested straight sample nets with varying SC, and sample nets with fixed SC but varying geometries affecting C_d.

4.3.1   Climatic wind tunnel.   In order to obtain controlled measurements of water collection rates, with similar conditions as the CFD simulations, a blow-down climatic wind tunnel was constructed. The tunnel was placed inside a climate room held at 100% relative humidity and an ambient temperature of 20 °C continuously. The wind tunnel consists of a settling chamber ($0.60m \times 0.60m$) filled with two layers of straighteners. Each straightener is $8.5mm$ long and consists of $15mm \times 15mm$ squares. The settling chamber is followed by a contraction cone and the test section with a surface area of $0.30m \times 0.30m$ and a length of $0.60m$. At the inlet of the tunnel, a nozzle driven by pressurized air (Cumulus, model CI-2) provides a stable fog stream with suspended water droplets ranging from 20 to $40\,\mu m$. The velocity of the undisturbed fog stream was determined inside the test section with an ONSET 3 cup anemometer measuring a constant velocity of $3.7m/s$. The liquid water content of the stable fog stream flowing through the wind tunnel test section is unknown. A schematic diagram of the climatic wind tunnel is given in figure 3. Building instructions are available in Goense (2018).

Figure 3. Schematic diagram of the wind tunnel for the fog collection experiment in the climate room.

4.3.2   Sample preparation.   Six straight sample nets of varying shade coefficients were 3D printed on a Anet A8 3D printer using PLA filament, see figure 4. Each net consists of a square frame of cylinders with a diameter of $4mm$ and a torus with a diameter of $12mm$ at each corner for suspension. The space within the frame ($100mm \times 100mm$) was filled with filaments with a diameter of $1.3mm$. The CFD analysis does not take drainage and clogging effects into account. Previous lab experiments have shown that harp-like fog harvesters have significantly less clogging issues and higher drainage efficiencies (Shi et al., 2018). The numerical 2D geometries of the CFD experiments consist of solid circular bodies and are best represented in the sample as cylinders. Therefore, round filaments were used as frame filling. Each net has a different number of equally spaced filaments in order to vary the shade coefficient. The shade coefficients are defined as in paragraph 2.2.3.

Figure 4. Example schematic of the 3D printed fog harvester samples. a) Shows an example of a straight FWC sample with an SC of 50%. b) Shows an FWC sample with a parabolic geometry, built up out of five parts with a curve extruding 50mm.

Two nets with a parabolic geometry, and an SC of 0.50, were printed in order to produce samples with varying drag coefficients. Both nets have a total frontal area of $100mmx100mm$ and a similar frame to the straight FWCs of $4mm$ cylinders providing the filaments with support. One net has a curve extruding $20mm$ and the other one of $50mm$, creating geometries similar to those of the simulations, as shown in figure 2. We printed the parabolic samples in five parts that were joined together afterwards, see figure 4 for an example of the sample with an extrusion of 50mm. The nets were either

used as a concave or a convex geometry, by changing their facing direction in the wind tunnel.

The Reynolds number of the samples suspended in the wind tunnel is approximately $1.3 \cdot 10^3$, which is large enough such that C_d does not change significantly compared to the CFD model or larger fog harvesting devices. The C_d of the samples was computed using the CFD simulations, see table 3.

We suspended the samples in the middle of the frontal area of the test section at $0.40m$ from the outlet of the tunnel. The samples cover 12% of the total surface area of the tunnel, leaving sufficient space for air to flow around the sample and not be affected by blockage (Barlow, Rae, & Pope, 1999). Samples are suspended by elastic bands with the filaments positioned vertically to enhance drainage.

Water is captured via a slanted (8°) 3D printed plate at the bottom of the tunnel leading towards a drain from which water runs to an ONSET tipping bucket rain gauge that is covered to avoid extraneous water from entering, see figure 3. For each sample, the water collection rate was measured for 20 minutes.

Table 1

Summary of flow velocity (v), wire diameter (D_w), and droplet diameter (D_d) for the analytical model and CFD model used in this study to compare droplet deposition on a single cylinder.

	Analytical Model	CFD Model	Experiments
$v\ (m/s)$	4	4	-
$D_w\ (mm)$	1	1	-
$D_d\ (\mu m)$	$0.1 \leq D_d \leq 1000$	$1; 5; 10;$	-
		$20, 50; 100$	-

5   Results

The fog collection efficiency was analysed for three different scenarios: 1. single cylinder with varying droplet diameter; 2. varying SC; and 3. varying C_d, using the analytical and CFD model. For every scenario one parameter was varied; hence, the influence of one parameter could be evaluated. For scenario 2. and 3. experiments in

Table 2

Summary of flow velocity (v), shade coefficient (SC), wire diameter (D_w), and droplet diameter (D_d) for the analytical model, the CFD model and the experiments used in this study to compare water collection of straight FWCs with varying SC.

	Analytical Model	CFD Model	Experiments
$v\,(m/s)$	4	4	3.7
$D_w\,(mm)$	1	1	1.3
$D_d\,(\mu m)$	10	10	$20 \leq D_d \leq 40$
$SC\,(-)$	$0.2 \leq SC \leq 0.9$	0.20; 0.25; 0.28;	0.19; 0.29; 0.39;
		0.33; 0.40; 0.44;	0.50; 0.59; 0.75
		0.50; 0.58; 0.61;	
		0.67; 0.72; 0.77;	
		0.80; 0.87; 0.91	

the climatic wind tunnel were performed to validate the results of the CFD calculations. An overview of all relevant parameters is given in tables 1, 2, and 3.

5.1 CFD Model

5.1.1 Droplet deposition on a single cylinder. The droplet deposition efficiencies on a single cylinder are plotted on a logarithmic scale for the analytical and CFD model, and are given in figure 5. When only one cylinder is considered, we assume that the analytical model only consists of equation (3) and the aerodynamic efficiency is 1. Both the analytical model and the CFD analysis show a clear sigmoid curve. The CFD model shows slightly higher efficiencies than the analytical model of Langmuir and Blodgett (1946), especially for the larger droplet diameters.

5.1.2 Effect of SC on collection efficiency. The fog collection efficiencies of a straight FWC with varying SC are plotted in figure 6. Both models show a concave downward parabola. According to the analytical model, the maximum water collection rate is reached for SC 0.49 to 0.61, with an efficiency of around 0.21. For the CFD model, the highest efficiency is 0.24, for a net with an SC of 0.50. For the lower SCs, 0.2 to 0.33, the analytical and CFD model predict similar values. However, as SC gets larger the CFD predicts larger efficiencies, the biggest difference is found for the FWC

15

Table 3

Summary of shade coefficient (SC), flow velocity (v), droplet diameter (D_d), and drag coefficient (C_d for the analytical model, CFD model and experiments used in this study to compare water collection of FWCs with varying shapes.

	Analytical Model	CFD Model	Experiments
$SC\,(-)$	0.6	0.6	0.5
$Effective\ SC\,(-)$	0.6; 0.65; 0.75	-	-
$v\,(m/s)$	4	4	3.7
$D_d\,(\mu m)$	10	5; 10; 50	$20 \leq D_d \leq 40$
$C_d\,(-)$	0.3 - 1.5	0.41; 082; 0.92;	0.41; 0.79; 0.89;
		0.97; 1.37	1.09; 1.27

with an SC of 0.77, where the efficiency of the CFD is a factor 1.28 higher than the analytical model.

5.1.3 Effect of FWC shape on collection efficiency. While the analytical model predicts an decreasing collection efficiency with lower C_d, the results of the CFD model remarkably show that concave shaped FWCs, with low C_d, have higher collection efficiencies than the straight FWC. The computational fog collection efficiencies of the FWC geometries as presented in figure 2, are plotted in figure 7 together with the results from the analytical model. The blue line represents the analytical model as it is described in equation (4), applying a value of 0.6 for the SC. In this case, the model shows a clear decline for smaller drag coefficients. However, In the CFD model, collection efficiencies of the two convex shapes, $C_d = 0.81$ and $C_d = 0.41$, are a factor 1.44 and 1.43 larger than the efficiency of the straight net.

In equation (4), SC represents the fraction of frontal surface area that is covered by net wires, i.e. the fraction on which droplets can deposit. Because of the parabolic shape of the convex and concave geometries the effective SC on which droplets can deposit is larger than that of the net. Therefore, we applied the analytical model to the five geometries adjusted for the effective SC. We define the effective SC as the fraction of the frontal area that would be covered if all the net wires were aligned. We determined the average effective SCs from the digital geometry files of the CFD simulations. The parabolic geometry with a curve extruding $0.50m$ has an effective SC
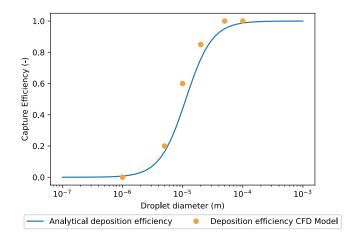
Figure 5. Analytical model for the deposition efficiency (η_d, equation (3)), and the impaction efficiency of a single cylinder according to the CFD model, as function of droplet diameter. Deposition efficiency increases as droplet size increases up to a maximum where all droplets heading towards the cylinder will deposit, producing an S-curve.

of 0.75, and the geometry extruding $0.20m$, 0.65. We used the net characteristic SC to calculate the pressure drop coefficient in equation (4).

For the analytical model where the effective SC is applied, collection efficiencies of the two convex shapes, $C_d = 0.81$ and $C_d = 0.41$, are a factor 1.04 and 0.96 factor different from the efficiency of the straight net, respectively.

Figure 8 shows the five different simulated geometries, but now simulated for three different droplet sizes. According to the simulations of a single cylinder, the deposition efficiencies for droplets with a diameter of $5\,\mu m$, $10\,\mu m$, and $50\,\mu m$ are 0.28, 0.61, and 0.97, respectively, see figure 5.

For the slightly convex shape ($C_d = 0.82$), we see an increase in collection efficiencies for each droplet diameter larger than the factor increase of 1.04 expected from the analytical model. For the droplets with a diameter of $5\,\mu m$ the relative increase compared to the straight FWC is a factor 2.00. For $D_d = 10\,\mu m$ and $D_d = 50\,\mu m$ the increase is with a factor 1.44 and 1.26 respectively.

For the shape with the smallest drag coefficient ($C_d = 0.41$) the efficiencies change, relative to the FWC with $C_d = 0.81$, with a factor 1.16, 0.99, and 0.85 , for
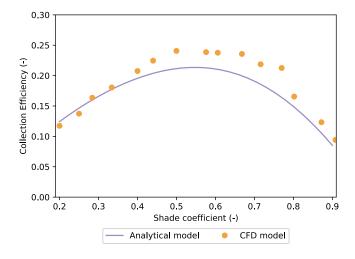
Figure 6. Fog water collection efficiency as predicted by the analytical model (η_c, equation (4)), and the CFD model, for straight FWCs as a function of SC. In both models, efficiency increases up to a maximum around SC=0.5, after which it declines again.

droplets with a diameter of 5 μm, 10 μm, and 50 μm, respectively.

As the analytical model predicts, the FWC with the largest drag coefficient has the largest increase in efficiency. For the concave shapes the relative increase compared to the straight FWC is largest for the smallest droplets. For the droplets with a diameter of 5 μm the relative increase compared to the straight FWC is a factor 2. For $D_d = 10\,\mu m$ and $D_d = 50\,\mu m$ the increase is a factor 1.6 and 1.5, respectively.

5.2   Experimental results

5.2.1   Straight sample FWCs.   The fog collection rates of six FWC samples with varying SCs were tested in a climatic wind tunnel as described in section 4.3.1. Figure 9 shows the water collection rates for each sample based. The raw data is available as supplementary material. The differences in fog collection rates were tested by an unpaired t-test. The test results of p < 0.0005, indicate the differences measured are very unlikely to be caused by random variations.

From the analytical and CFD model we expect there to be a rise in water collection rates as SC increases up to a certain point, after which the collection rate
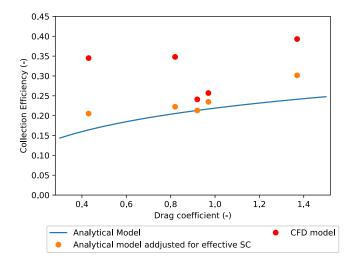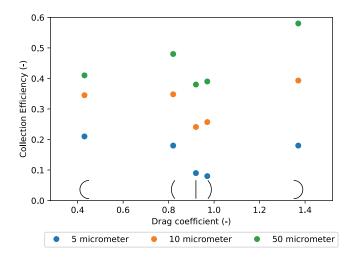
Figure 7. Fog water collection efficiency as predicted by the analytical model (η_c, equation (4)), the analytical model adjusted for effective SC, and the CFD model, for FWCs with varying drag coefficients and an SC of 0.6. All four parabolic shapes have a higher collection efficiency than the straight FWC. The analytical model predicts a decline for smaller drag coefficients, even when adjusted for effective SC. The results of the CFD model show higher collection efficiencies for the concave FWCs than the straight FWC.

declines rapidly. The results in figure 9 show the same pattern as figure 6. With a water collection rate of $52.6 \pm 3.4 \, L/m^2h$, the sample with a shade coefficient of 50% harvests the most water from the fog stream. The samples with the lower SCs of 20%, 30%, and 40% have a collection rate of $21.8 \pm 3.1 \, L/m^2h$, $25.8 \pm 2.7 \, L/m^2h$, and $39.0 \pm 3.5 \, L/m^2h$, respectively. The samples with the higher SCs of 60% and 75% have a collection rate of $33.8 \pm 6.3 \, L/m^2h$ and $14.4 \pm 5.8 \, L/m^2h$, respectively.

During the experiments, we noticed that the two FWCs with the largest SC showed different drainage behaviour than the other FWCs. Water droplets stayed adhered in between the filaments of the sample, whereas with the other FWCs the droplets drained down along the filament.

5.2.2 Concave and convex sample FWCs. The fog collection rates of 3 FWC samples with varying shapes were tested in a climatic wind tunnel as described in section 4.3.1. The straight FWC was tested once for each experiment round. The two
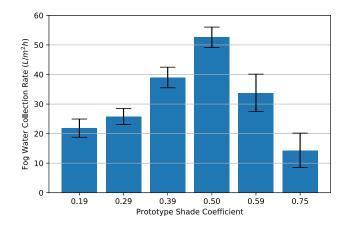
Figure 8. Fog water collection efficiency as predicted by the CFD model for three different droplet diameters, for FWCs with varying drag coefficients and an SC of 0.6. For smaller droplets diameters the relative increase in efficiency compared to the straight FWC is larger than for larger droplets.

parabolic FWC samples were tested twice, once as a convex shape and once as concave shape. Thus in total five different drag coefficients were tested consecutively, this was repeated three times.

The data of all three experiments is joined together and presented in figure 10, showing the water collection rates for each sample. The raw data is available as supplementary material. The differences in fog collection rates were tested by an unpaired t-test. The test results of $p < 0.0005$, indicate the differences measured are very unlikely to be caused by random variations.

Each experiment showed a higher collection rate, per unit of frontal area, for the parabolic shapes than for the straight FWC. The straight FWC has a collection rate of $61.2 \pm 8.8 \ L/m^2h$. The convex FWCs with drag coefficients of 0.41, and 0.79 have collections rates of $82.7 \pm 9.5 \ L/m^2h$, and $66.4 \pm 14.6 \ L/m^2h$, respectively. The concave FWCs with drag coefficients of 1.09, and 1.266 have collections rates of $77.8 \pm 10.0 \ L/m^2h$, and $97.4 \pm 14.9 \ L/m^2h$, respectively.

In figure 10 b) the water collection rates are adjusted for the increase in net area of the parabolic shapes. The differences in fog collection rates were tested by an

Figure 9. Fog water collection rates tested for 20 minutes for six straight FWC samples with varying SC. The performance of the samples improves as SCs becomes larger, and reaches a maximum for the sample with an SC of 50%. For the two higher SCs the collection rate declines. This pattern is also predicted by the analytical model and CFD model.

unpaired t-test. For the FWC samples with a drag coefficient of 0.41 and 1.09, the test results of $p < 0.0005$, indicate the differences measured compared to the straight sample are very unlikely to be caused by random variations. Water collection rates per unit area of net increase with a factor 1.19 for the slightly concave shape ($C_d = 1.09$). For the shapes with drag coefficient 0.86 and 1.266, p values are 0.25 and 0.12, indicating the differences measured are likely to be caused by the increase of net area instead of the change in shape.

6   Discussion

6.1   Droplet deposition on a single cylinder

The results of the CFD model showed that fog collection efficiency is strongly influenced by the droplet size of the fog. Deposition efficiency increases as droplet size increases up to the maximum where all droplets heading towards the cylinder will deposit, producing an S-curve (see figure 5). The results compare well to the analytical model based on the formula for deposition efficiency of Langmuir and Blodgett (1946).
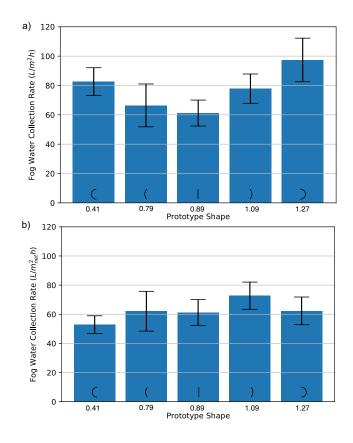
Figure 10. Fog water collection rates tested for 20 minutes for five different geometries with an SC of 0.5. a) Shows the water collection rates for each geometry as measured by the tipping bucket. There is a clear increase for each for each parabolic sample compared to the straight sample. The increase by the concave shapes is larger than for the concave shapes. b) Shows the collection rates per m^2 of sample net. The results show that for the slightly concave shape there is a significant increase in water collection.

6.2   Varying SC of straight FWCs

The analytical model for aerodynamic efficiency as proposed by Rivera (2011) predicts that there is a maximum fog water collection efficiency for SCs between 0.5 and 0.6. The CFD simulations for a straight FWC with varying SC shows a maximum around an SC of 0.5. However, predicted efficiency values for FWCs with an SC of 0.3 to 0.77 become progressively larger than the analytical model suggests, after which differences become smaller again. Rivera (2011) already points out that the analytical model for aerodynamic efficiency is an indication of the where the maximum is and does

not strive to determine exact values for the aerodynamic efficiency. From the CFD simulations, we observed that water collection is not homogeneous over the net area, and as SC increases, relatively more water is collected at the edges of the FWC. This suggests that, when scaling to larger fog harvesting devices efficiencies might differ.

These results were confirmed during the controlled experiments in the climatic wind tunnel. For the sample with an SC of 0.50 we observed the largest collection rate. During the experiments we observed that droplets stayed suspended in between the filaments for the samples with an SC of 0.6 and 0.75, while for the other samples droplets glided down along the filament as soon as a critical droplet volume was reached. This can explain the larger than expected drop in collection rate for the samples with higher SC compared to the analytical and CFD model. Suggesting that during lab experiments drainage efficiency does play a role.

These experimental results, which are important and relevant for the development of more efficient FWCs, have never been demonstrated before. Field tests have been performed comparing different meshes (Fernandez et al., 2018; Schunk et al., 2018), however nets differ from each in more ways than just SC, making it hard to draw the same results from these studies.

6.2.1 Varying shape of FWCs. We tested the influence of geometry on the water collection potential of fog harvesting devices. We analysed five different shapes, thus varying the drag coefficient of the collector. Whether the shape was placed concave or convex facing the fog stream, all four parabolic shapes were found to be more advantageous than the straight FWC. These results were observed in the CFD simulations and confirmed by the experiments of the curved samples in the climatic wind tunnel. When the analytical model is adjusted for the effective SC, the two concave shapes, i.e the FWC with the higher drag coefficient, do predict an increase in efficiency, but not as pronounced as the CFD model.

For the two concave shapes, the enhanced fog collection is caused by the higher drag coefficient, as was discussed in Rivera (2011). The pressure difference for the air to go around the FWC becomes larger as the drag coefficient increases and more air will

flow through the net, resulting in an increase in water collection. De la Jara (2012) found similar results with numerical simulations of V-shaped FWC in COMSOL Multiphysics. In de la Jara (2012), the opening of the V-shaped FWC was facing the incoming fog stream, and fog collection efficiency increased from 30% to 50% as the angle became more acute. Holmes et al. (2015) made use of the findings of the study of de la Jara (2012) to design a funnel shaped FWC. The study showed, using numerical simulations, that fog water collection efficiency could be increased from 24% for a straight FWC to 64% if a funnel shape was used.

The efficiencies of de la Jara (2012) and Holmes et al. (2015), are based on the frontal area of the FWC and not the total net area. This is relevant when considering the costs per unit water produced. Holmes et al. (2015) showed that the net area of the funnel shaped FWC is factor 1.76 larger than the conventional one, while the water collection efficiency increases by a factor 2.46. For the two concave shapes considered in this study the fog water collection efficiency nor increases, nor decreases, when adjusted for the increased net area, according to the CFD model.

The experimental results showed that the increase in water collection is highest for the only slightly concave sample ($C_d = 1.09$). While the shape with the largest drag coefficient showed little difference in water collection per unit of area net compared to the straight sample. One experiment did show a larger increase in water collection per unit net area for the concave shapes. During this experiment, we measured an increase of 1.46 and 1.22 for the samples with a drag coefficient of 1.09 and 1.27 per unit net area, respectively. It is hard to determine what caused these differences, absolute care was taken to keep the environment and experimental set up unchanged between experiments. However, also the single experiment shows the largest increase for the slightly concave sample. This suggest there is an optimum size for the curve inward for which the efficiency per unit net area is highest.

It is important to consider that the factor increase in net area is not equal to the factor increase in costs. The net is only fraction of the total cost of implementing FWCs. It might be more important to consider what the change in geometry means for

the overall sustainability of the device.

For convex shapes the analytical model, even adjusted for effective SC, predicts only a small increase in fog water collection relative to the conventional FWC, while the CFD model and experiments show a significant increase. These findings, which are important for the design of more efficient FWCs, have not been demonstrated before. The change in relative increase in water collection varies for different droplet diameters, suggesting that the deposition mechanism changes when the FWC is convex. The analytical model does not take this into account.

Close examination of the impaction behaviour in the numerical simulations reveal that water collection is not homogeneous over the net, and most droplets are captured by the net wires at the edges of the FWC. When the air flows around a straight FWC, once it has passed the structure is does not encounter any wires anymore. When the air tries to flow around a convex structure, each time a droplet has avoided a net wire, it is confronted with another one behind it and at some point the droplet is impinged on a net wire. Although less air passes through the net due to it's low drag coefficient, deposition efficiency increases. In the simulation results, figure 7, we found that this increase is more pronounced for smaller droplets. This could be caused by the fact that for droplets with a smaller diameter the deposition efficiency on a single cylinder is smaller than for larger droplets, see figure 5. For larger droplets, deposition efficiency is almost 1, and the increase in efficiency is only caused by the change in shape. Whereas for the smaller droplets the deposition efficiency on a single cylinder is 0.28 and the increase is caused by a combination of change in shape and increase in deposition efficiency.

The wind tunnel experiments show the increase for the convex shapes to a lesser extent than the CFD model. When the change in impaction area is taken into account it seems that the increase in water collection is caused by an increase in impaction area, see figure 10 b). The influence of droplet size could not be validated during the experiments because the nozzle available in this research could not be adjusted. This nozzle produces droplets in the range of 20 to 40 μm according to the nozzle

specifications. Slightly larger than the concentration peak of 10 μm found at fog sites, but covering part of the 2 to 30 μm range (Schemenauer & Joe, 1989). The relatively large droplet size and small sample scale could have lead to an already high deposition efficiency during the experiments and explain why the results from the CFD model are different. Field experiments are advised to further compare the results of the CFD model.

Besides a potential increase in water collection, the convex shapes have two additional advantages over the straight FWC. First of all, the structural integrity of the fog harvesting device will improve because a lower drag force will act upon the whole device. To built a convex FWC smaller mesh areas between the supporting frames are necessary, decreasing the strain on the mesh and the probability of ruptures (Holmes et al., 2015). Secondly, the convex shapes with lower drag coefficients, especially when made round, are less dependent on wind direction.

7   Conclusion

We have demonstrated, using CFD simulations and confirmed with wind tunnel experiments, that deposition efficiency is affected when changing the geometry of the fog water collector. This differs from the analytical models previously used in Rivera (2011), Park et al. (2013), and Regalado and Ritter (2016) to theoretically predict efficiency. Building fog water catchers convexly facing the wind can collect more fog water than previously expected, this means that more cost-effective fog harvesters can be built that are better equipped for withstanding the force of the wind. An analytical model that could take these findings into account is now an open research opportunity. Further research on large FWCs in the field is necessary to confirm the advantages of convex FWCs and investigate if CFD simulations and testing prototypes in a small-scale wind tunnel are effective design tools for fog water harvesting devices. This research is a first step that will lead to reliable and economically feasible fog harvesters with high efficiency.

8   References

Azad, M. A. K., Ellerbrok, D., Barthlott, W., & Koch, K. (2015). Fog collecting
    biomimetic surfaces: Influence of microstructure and wettability.
    doi: 10.1088/1748-3190/10/1/016004

Barlow, J., Rae, W., & Pope, A. (1999). *Low-Speed Wind Tunnel Testing.*

Batisha, A. F. (2015). Feasibility and sustainability of fog harvesting. *Sustainability of
    Water Quality and Ecology*, *6*, 1–10. doi: 10.1016/j.swaqe.2015.01.002

de la Jara, E. A. (2012). *Modelacion computacional del impacto de gotas de niebla en
    fibras cilindricas paralelas* (Tech. Rep.). Santiago de Chile: Pontifica Universidad
    Catolica de Chile.

Ebner, M., Miranda, T., & Roth-nebelsick, A. (2011). Efficient fog harvesting by
    Stipagrostis sabulicola (Namib dune bushman grass). *Journal of Arid
    Environments*, *75*(6), 524–531. doi: 10.1016/j.jaridenv.2011.01.004

Fernandez, D. M., Torregrosa, A., Weiss-penzias, P. S., Zhang, B. J., Sorensen, D.,
    Cohen, R. E., . . . Park, M. (2018). Fog Water Collection Effectiveness : Mesh
    Intercomparisons. , 270–283. doi: 10.4209/aaqr.2017.01.0040

Goense, A. L. (2018, Jul). *Climatic wind tunnel.* Instructables. Retrieved from
    `https://www.instructables.com/id/`
    `Climatic-Wind-Tunnel/`

Hahner, F., Dau, G., & Ebert, F. (1994). Inertial Impaction of Aerosol Particles on
    Single and Multiple Spherical Targets. , *17*, 88–94.

Holmes, R., Rivera, J. d. D., & de la Jara, E. A. (2015). Large fog collectors: New
    strategies for collection efficiency and structural response to wind pressure.
    Atmospheric Research, *151*, 236–249. doi: 10.1016/j.atmosres.2014.06.005

Idel'chik, I. E. (1960). *Handbook of hydraulic resistance (3rd edition).* doi: AEC-tr-
    6630

Israel, R., & Rosner, D. E. (1982). Use of a generalized stokes number to determine the
    aerodynamic capture efficiency of non-stokesian particles from a compressible gas
    flow. *Aerosol Science and Technology*, *2*(1), 45–51.

Klemm, O., Schemenauer, R. S., Lummerich, A., Cereceda, P., Marzol, V., Corell, D., . . . Frost, E. (2012). Fog as a Fresh-Water Resource : Overview and Perspectives. , *1998*, 221–234. doi: 10.1007/s13280-012-0247-8

Langmuir, I., & Blodgett, K. B. (1946). A mathematical investigation of water droplet trajectories. , 348–393.

Park, K. C., Chhatre, S. S., Srinivasan, S., Cohen, R. E., & McKinley, G. H. (2013). Optimal design of permeable fiber network structures for fog harvesting. *Langmuir*, *29*(43), 13269–13277. doi: 10.1021/la402409f

Regalado, C. M., & Ritter, A. (2016). The design of an optimal fog water collector: A theoretical analysis. *Atmospheric Research*, *178-179*, 45–54. doi: 10.1016/j.atmosres.2016.03.006

Regalado, C. M., & Ritter, A. (2017). The performance of three fog gauges under field conditions and its relationship with meteorological variables in an exposed site in Tenerife (Canary Islands). *Agricultural and Forest Meteorology*, *233*, 80–91. doi: 10.1016/j.agrformet.2016.11.009

Regan, B. D., & Raynor, P. C. (2009). Single-fiber diffusion efficiency for elliptical fibers. *Aerosol Science and Technology*, *43*(6), 533–543. doi: 10.1080/02786820902777215

Rivera, J. D. D. (2011). Aerodynamic collection efficiency of fog water collectors. *Atmospheric Research*, *102*(3), 335–342. doi: 10.1016/j.atmosres.2011.08.005

Schemenauer, R. S., & Cereceda, P. (1992). The quality of fog water collected for domestic and agricultural use in chile. *Journal of Applied Meteorology*, *31*(3), 275âĂŞ290. doi: 10.1175/1520-0450(1992)031<0275:tqofwc>2.0.co;2

Schemenauer, R. S., & Joe, P. I. (1989). The Collection Efficiency of a Massive Fog Collector. , *24*, 53–69.

Schunk, C., Trautwein, P., Hruschka, H., Frost, E., Dodson, L., Derhem, A., . . . Menzel, A. (2018). Testing Water Yield Efficiency of Different Meshes and Water Quality with a Novel Fog Collector for High Wind Speeds. , 240–253. doi: 10.4209/aaqr.2016.12.0528

Shi, W., Anderson, M. J., Tulko, J. B., Kennedy, B. S., & Boreyko, J. B. (2018). Fog
Harvesting with Harps.
doi: 10.1021/acsami.7b17488

Wahab, S. A. A., Lea, V., Abdul-wahab, S. A., & Lea, V. (2008). Reviewing fog water
collection worldwide and in Oman. , *7233*(May). doi: 10.1080/00207230802149983

White, B., Sarkar, A., & Kietzig, A. (2013). Applied Surface Science Fog-harvesting
inspired by the Stenocara beetle âĂŤ An analysis of drop collection and removal
from biomimetic samples with wetting contrast. *Applied Surface Science*, *284*,
826–836. doi: 10.1016/j.apsusc.2013.08.017

3. CFD simulation for fog water collection analysis

This chapter elaborates on how computational fluid dynamics were used during this study for analysing fog water catchers and how this method could be used for future design studies.

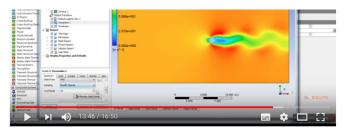tags: #CFD simulation #ANSYS Fluent #nice visuals #Stokes #design tool

During this project, computational methods were used to investigate the influence of shade coefficient, fog water catcher geometry, and fog droplet size on the water collection efficiency of fog harvesters. Numerical experiments give you the flexibility to analyse a vast amount of configurations, without spending the many resources that are required for physical tests.

We used ANSYS Fluent, a commercially available computational fluid dynamics (CFD) solver, to perform the numerical simulations. The solver predicts the fluid flow by solving a set of governing mathematical equation numerically. In the case of modeling the fluid flow behaviour for fog harvesting, the conservation of mass and momentum equations have to be solved. The fluid can be considered incompressible because of the low wind speeds.

The ANSYS solver is based on the finite volume method, which means that the physical system is discretized into a finite set of control volumes and the equations are solved on this set of control volumes. As the figure below shows, the modeling process is iterative, it starts with an initial guess of the solution and then uses the algebraic system of equations to correct, this is repeated until the solution is converged.
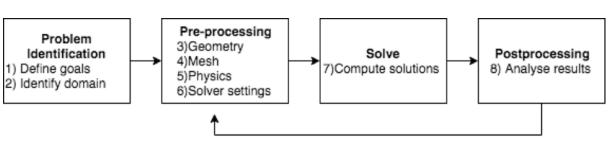
Steps to set up ANSYS Fluent model for fog water collection (pre-processing):

1. Simplify the physical system to 2D and set up the computational domain

2. Divide the domain into control volumes with the meshing tool

3. Set up the physical models that have to be solved, add a discrete phase model to represent the water droplets, and determine settings of the solver

4. Compute solution

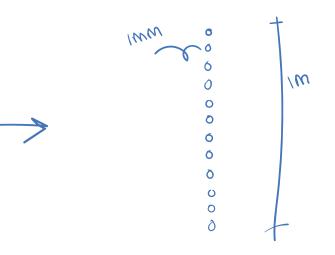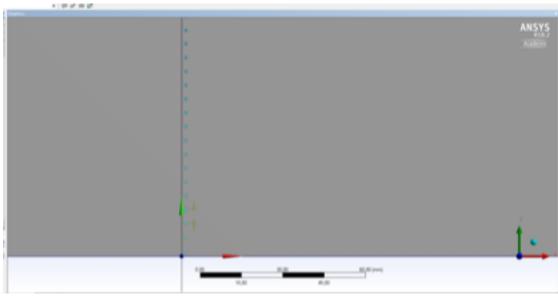ANSYS Fluent CFD Tutorial - Flow Over a Cylinder - Von Karman Animation

245,077 views   👍 1.6K   👎 25   ➔ SHARE   ⯇+   •••

super helpful tutorial

ANSYS Fluent modeling overview.
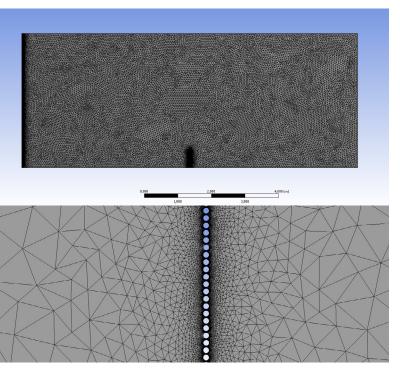
Computational domain

We simplified the fog catcher in 2D as a collection of circles representing the net wires. The distance between the circles and the positioning determined the shade coefficient and overall geometry. In this study, we chose circles of 1mm and a total frontal length of 1m.

Printscreen of ANSYS Fluent design modeler showing part of the computational domain, zoomed in on the circles representing the net wires.

Mesh generation

After we defined the physical domain, we created the mesh, dividing the domain into control volumes on which the model equations can be solved. We used the mesh generation tool provided by the ANSYS software package. The aim is to do sound computations with the minimum amount of control volumes. Therefore, the mesh was not homogenous over the domain; small volumes were placed at the boundaries of the fog catcher wires and the inlet. In the rest of the domain, we used larger volumes. We performed a mesh convergence study for the fog catcher with a shade coefficient of 90%. The final mesh had an overall maximum element size of 0.1m, at the inlet elements of 0.0005m, and around the fog catcher wires elements of 0.00005m, using triangular elements as shown in the figures on the right.

Solver settings

In this study, we used the Reynolds-averaged Navier-Stokes (RANS) method. The method assumes that most turbulent flows have an average and that it is their average you are most interested in and not their fluctuations. This method gives you a time-averaged solution, and terms for turbulence are approximated with a turbulence model. During this project we used the k-e turbulence model, k is a measure of kinetic energy and e of the rate of dissipation.

Additionally to the transport equations a discrete phase model (DPM) was solved. The DPM introduces a second phase that consists of spherical particles, which in this case we used to represent the water droplets of the fog. The DPM provided us with the possibility to track the trajectory of the droplets taking into account the inertia of the droplet. The DPM assumes that there is not particle-particle interaction and that the effect of the particle volume fraction on the gas phase is negligible.

The discrete particles were injected from the domain inlet with the same velocity as the air. The boundary condition at the fog harvester wires determined that as soon as a droplet would hit the wire it would be captured and no further interaction would take place. At the outlet, a pressure outlet condition was set, and droplets would escape.
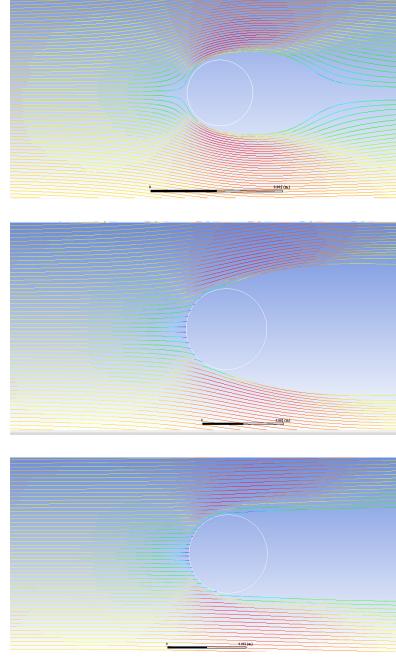
Visual results

Results of the computational simulations are extensively discussed in the academic paper. Here some of the visual results are presented to give an idea of what happens to the fog harvesting mechanism when the geometry of the catcher is adjusted.
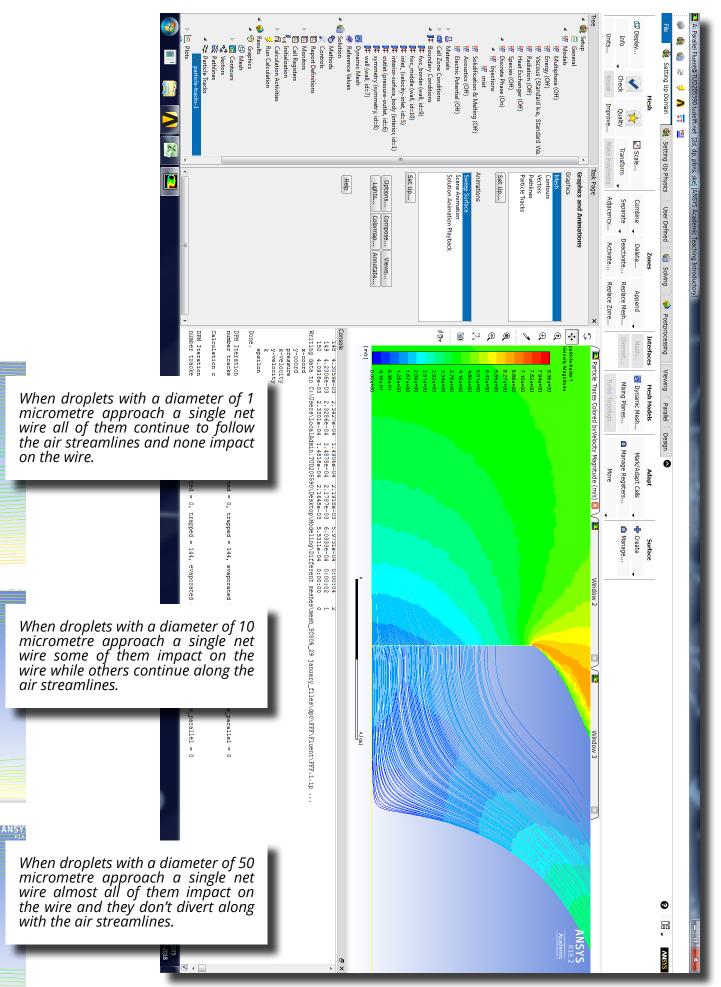
Impaction on a single cylinder

It has to be understood that whether or not a droplet will impact on a wire of a fog catcher net does not depend on the material of the net. When a droplet is suspended in an air stream heading towards a wire, it depends on the inertia of the droplet. Small particles will adjust to the sudden change of the air streamlines and will be carried around the wire, whereas larger particles will depart from the streamlines and impact on the wire. This phenomenon can be observed in the three figures on the right.

So changing the wettability of the mesh material will not influence the amount of water that is captured, only how it is drained of the net.

When droplets with a diameter of 1 micrometre approach a single net wire all of them continue to follow the air streamlines and none impact on the wire.

When droplets with a diameter of 10 micrometre approach a single net wire some of them impact on the wire while others continue along the air streamlines.

When droplets with a diameter of 50 micrometre approach a single net wire almost all of them impact on the wire and they don't divert along with the air streamlines.
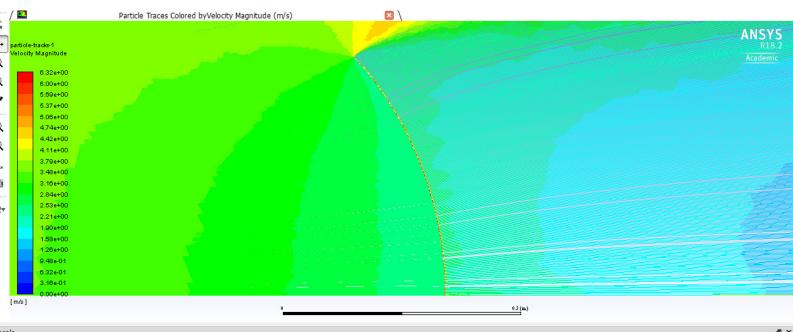
Printscreen of the user interface of the ANSYS Fluent solver set up after the solution has converged and the particle tracks are presented in the monitor.

Droplet deposition on curved fog harvesters

During this study, we found that convexly curved fog harvesters have a higher water collection efficiency than expected. The analytical model disregards convex fog harvesters because their lower drag coefficient reduces the aerodynamic efficiency of the fog harvester. The results of the CFD models show that efficiency can be doubled if fog catchers are built convex facing the wind. The results of this study indicate that for convex fog harvesters, although less fog passes through the net, the deposition efficiency increases resulting in a net increase of water collection.
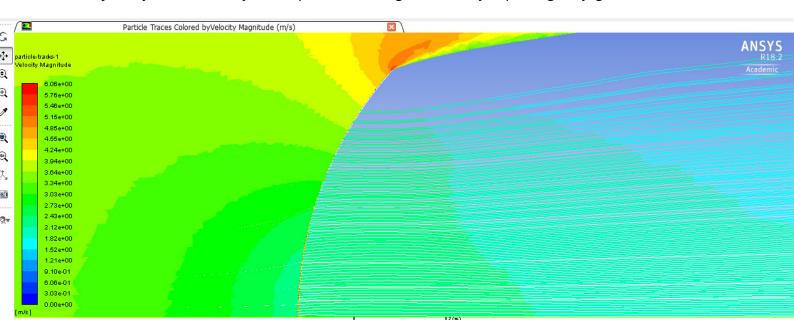
Within the scope of this project, it was not possible to fully delve into the mechanisms that cause the unexpected behaviour of convex fog catchers. However, an examination of the impaction behaviour in the numerical simulations can give us some valuable insights that could be explored during future research.
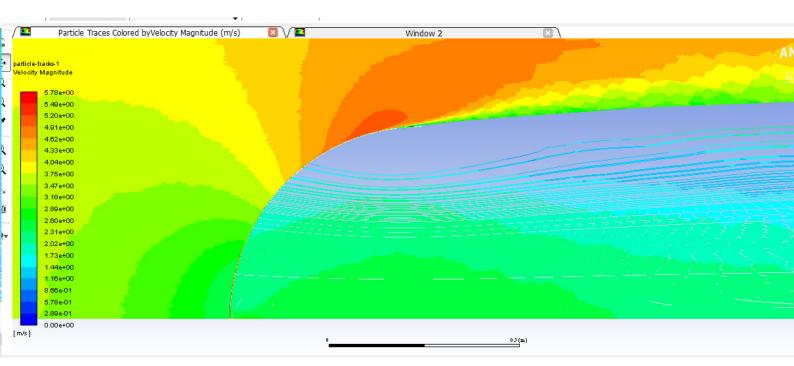

Printscreen of ANSYS Fluent particle tracking. Droplets with a diameter of 10 micrometre head towards a concave fog water catcher. The fog stream behind the fog catcher is less dense, but still homogenous in density. The flow direction of the droplets is diverting outwards after passing the fog catcher.

Printscreen of ANSYS Fluent particle tracking. Droplets with a diameter of 10 micrometre head towards a slightly convex fog water catcher. The fog stream behind the fog catcher is less dense, and at the edge no particles pass through the net.
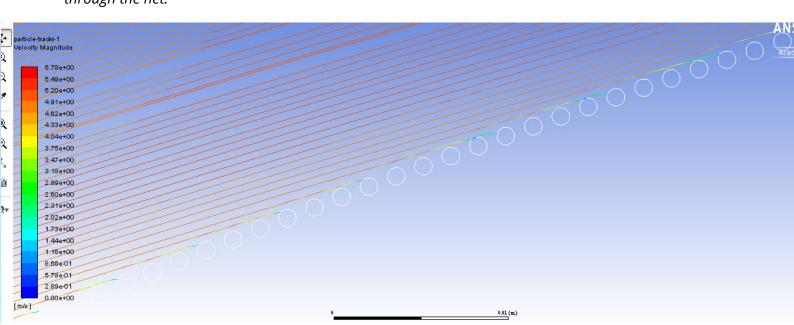
Printscreen of ANSYS Fluent particle tracking. Droplets with a diameter of 10 micrometre head towards a concave fog catcher. The fog stream behind the fog catcher is less dense, and at the edge no particles pass through the net.

Printscreen of ANSYS Fluent particle tracking zoomed in on concave fog catcher of the figure above. When the air tries to flow around a convex structure, each time a droplet has avoided a net wire, it is confronted with another one behind it and at some point the droplet is impinged on a net wire.

LOW-SPEED WIND TUNNEL TESTING

THIRD EDITION

Jewel B. Barlow
William H. Rae, Jr.
Alan Pope

methods leading to quantitative predictions have been a combination of experiment and theory, with computational methods becoming a new tool of increasing consequence since the 1960s. The great advances in theory and computational capability notwithstanding, experimental explorations remain the mainstay for obtaining data for designers' refined and final decisions across a broad range of applications. A primary tool of experimental aerodynamics is the wind tunnel. The proper and productive use of experimental investigations in general and wind tunnels in particular requires applications of aerodynamic theory and computational methods in the planning of facilities, the planning of experiments, and the interpretation of resulting data. Those aspects of aerodynamics will be drawn upon heavily in the course of this book.

To answer the question posed above: The invention, use, and ongoing evolution

4. How to build a climatic wind tunnel on a budget

Using an instructable as format this chapter explains how the wind tunnel used during this project was built.
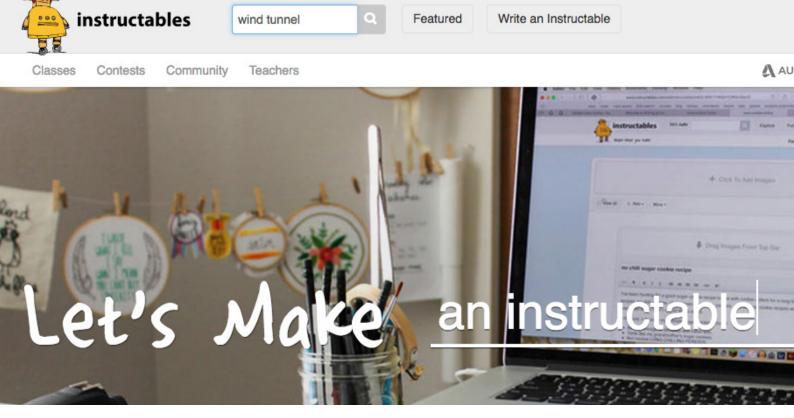
tags: #wind tunnel #budget #instructable #tutorial

It was necessary to build a climatic wind tunnel to test different fog catcher prototypes. A task I mostly felt confident about because of the enthusiasm of my supervisor Rolf Hut. I was in luck because the faculty of Civil Engineering and Geosciences at the TU Delft has a huge climate room used for curing concrete. The room kind of looks like a dirty men's locker room filled with concrete blocks and nozzles that permanently spray mist into the room to keep the relative humidity at 100%. This meant that at least I didn't have to concern myself with controlling the climate of the test setup. I only had to learn how wind tunnels work and design one that fitted my needs. In the end, I have used two different wind tunnel setups for my experiments. The first design will be discussed in the Instructable since it can be built with relatively cheap materials available in most places, thus relevant for a wider public. Whereas, the second set up is dependent on the climate room I worked in and is elaborated in the paper.

The purpose of your wind tunnel and your budget determine the design. I wanted to keep the costs as low as possible, so I didn't want to build a very large tunnel, yet not too small that scaling would become a problem. To keep the Reynolds and Stokes numbers in the right order of magnitude, wind speeds of 3 to 5 m/s and prototype dimension of 10cm x 10cm were necessary. The frontal area of the scale model should not cover more than 10% of the area of the test section. So I decided on a test section area of 30cm x 30cm and a length of 60cm to leave enough space for the wake to develop behind the prototype.

For small scale, low speed, wind tunnels, such as the one I mad, fans are often used to make the wind. Although the climate room was a godsend, it also meant that I could not work with anything that can't stand that kind of levels of wetness, such as an electrically powered fan. Luckily there is a hole in the wall of the climate room that exactly fits the outlet of a leaf blower.

With the method of wind-making and size of the test section decided, the rest of the design could be made. This will be further explained in the following Instructable. I spend about 300 euros to built everything.

Let's Make an instructable

(/member/lucy-flamingo/)
By **lucy-flamingo (/member/lucy-flamingo/)**

About: . More About lucy-flamingo » (/member/lucy-flamingo/)

Follow

Summary: This is an instructable for a blowdown, open circuit, climatic, wind tunnel driven by a leaf blower and provided by a fog stream produced by a garden humidifier.

The World Health Organization (WHO) estimates there are 844 million people who lack basic drink water services. The exploration of unconventional water resources that have not yet been utilized, such as the water in the air, is necessary to meet (future) water demands.

Fog harvesting is a low cost, low tech, drinking water solution for arid regions where fog occurs on a regular basis. Most fog water collectors consist of a large mesh-like screen held by poles or a frame, perpendicular to the wind-driven fog.

For my MSc. thesis project at the technical university of Delft I researched the aerodynamics of fog harvesters. I built a climatic wind tunnel with the purpose to validate CFD results. This instructable outlines the construction of the set up I used. This wind tunnel can be used to test the designs of future fog harvesters, or any other project where you need to test the interaction of a stream of water droplets and an object.

Your wind tunnel might not turn out exactly the same because you are working with a different purpose, circumstances or resources. This instructable can still serve as useful inspiration for anyone building their own wind tunnel.

Many thanks go to to the people over at Sciencebuddies and the Instructable user beltenebros of rLoop, for your designs have helped me a lot with constructing this tunnel.
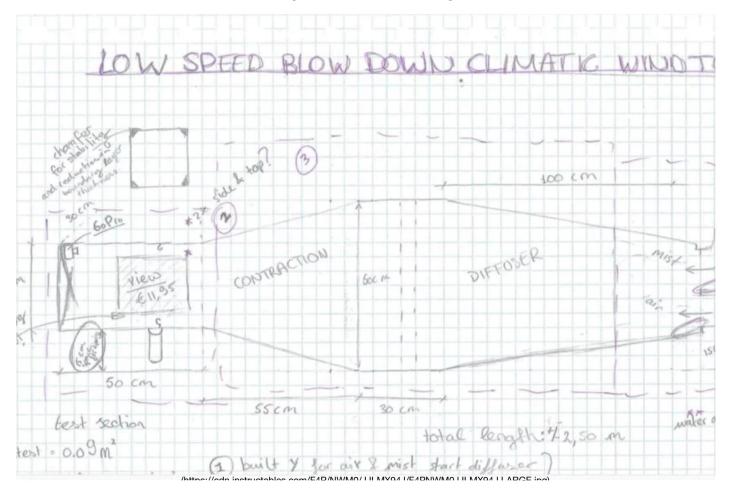
Sciencebuddies wind tunnel: https://www.sciencebuddies.org/science-fair-projec... (https://www.sciencebuddies.org/science-fair-projects/references/how-to-build-a-wind-tunnel#introduction)

rLoop: https://www.instructables.com/id/DIY-Subsonic-Wind... (https://www.instructables.com/id/DIY-Subsonic-Wind-Tunnel-LiftDrag-Testing-for-RLoo/)

If you would like have more in-depth knowledge on low speed wind tunnels, the book "Low speed wind tunnel testing" by Jewel B. Barlow, William H. Rae and Alan Pope, is a great resource.

Step 1: Overview Design

(https://cdn.instructables.com/F4P/NWM0/JHLMX94J/F4PNWM0JHLMX94JLARGE.jpg)

The two most basic things needed to build a wind tunnel are something that makes wind and some sort of tunnel. In the case of this setup, also a fog stream has to be introduced.

The purpose of your tunnel and your budget will largely determine your design. I wanted to keep the costs as low as possible, so I didn't want to build a very large tunnel, yet not too small that scaling would become a problem. To keep the Reynolds and Stokes numbers in the right order of magnitude, wind speeds of 3 to 5 m/s and prototype dimension of 10cm x 10cm are necessary. The frontal area of the scale model should not cover more than 10% of the area of the test section, this means the test section should be at least be 30cm x 30cm. I decided on a length of 60cm to leave enough space for the wake to develop behind the prototype.

39

For small scale, low speed, wind tunnels, such as the one made here, fans are often used to make the wind. Although the climate room I could work in was a godsend, it also meant that I could not work with anything that can't stand that kind of levels of wetness, such as an electrically powered fan. Luckily there was a hole in the wall of the climate room that exactly fits the outlet of a leaf blower.

The wind tunnel consists of five parts: the inlet, a diffuser, a straightener, a contraction cone, and the test section.

From the sketch on the wind tunnel, you can get a rough idea on the measurements. The ratio between the different parts is most important, the measurements can depend on your purpose and available budget.

Add Tip   Ask Question   Comment   Download

Step 2: Materials

(https://cdn.instructables.com/FDR/DFHL/ LJLMXC41/FDRDFHL LJLMXC41 LARGE.jpg)

Materials:

* leafblower *(Check in the specifications if the provided power will be sufficient, most manufacturers provide you with the wind speed and outlet area, you can use this information to estimate the discharge and wind speed in you test section, take into account that some losses will occur)*

* tropical plywood *(I specifically used tropical wood because it is better resistant to water)*

* triangular beams for connecting the corners *(Triangular because this causes less disruption of the air stream than rectangular beams)*

* wood dye/staining to make water resistant

* 40cm x 20cm plexiglass

* 1 garden hose sprinkler mist system --> see picture

It is estimated that these low-pressure mist systems produce droplets with a size of about 100 micrometres, pressurized nozzles will produce smaller droplets.

* 2x egg crates

* screws

* wood glue

* 16 springs

* air sealing strip

* 1 role of duct tape

* 4 hook screws

* tie wraps

* double-sided tape

maybe (depending on your purpose and location):

* flexible air ventilator tube

* rain gauge

tools
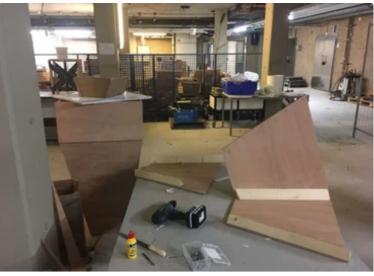
* jig saw

* drilling machine

Add Tip   Ask Question   Comment   Download

Step 3: Diffuser, Straightener and Contraction Cone

2 More Images

These three sections are the most straightforward to build, so a good place to start. All three follow a similar process, the only difference is that you need to add the egg crates to the straightener section.

The diffuser is there to make the air stream coming out of the leafblower wider and mix with the water droplets. In the straightener, turbulence is removed from the incoming air at a lower speed with the egg crates. In the contraction cone, the air is accelerated again and pressure differences are removed.

1) Saw the plywood and beams to size --> see sketch

2) Connect each of the four boards that belong to one section to create a tunnel form. I did this by first glueing one beam to two boards and let it dry. And then do the other two boards with another board. Then place the two L shapes together with the last two beams. It is nice to do this together with another person but not necessary.

After it is all glued together reinforce the connection with screws. Make sure to pre-drill.

4) Make the section water resistant with some sort of wood seal or dye and let it dry overnight. Add an extra layer for security if you have the time.

5) To make sure the wind tunnel has a modular set up that is easily taken apart and moved around the sections are connected with springs. Therefore add screws on the outside of all the corner edges so the springs can hook behind them. Think about the alignment between the different section. (In one of the pictures you can see what it is supposed to look like in the end).

6) Because the sections won't fit together perfectly you can add airstrips to all the edges to compensate for the slight irregularities. If your airstrip is a bit wider or thinner than the plywood plate it is not a big problem, just make sure the inside edges are aligned to avoid disruption of the air stream.

At last, you need to add the egg crates to the straightener. Cut or saw the egg crates to the right size, cut the corners off to fit with the beams. I placed each egg crate at 1/3, equally spacing them, in the straightener. If you cut them to be a good fit they already jam a bit, I added high quality (i.e. able to withstand a lot of water) double-sided tapes to keep them in place.

🔅 Add Tip   ❓ Ask Question   💬 Comment   Download

Step 4: Test Section

Depending on the use of your wind tunnel your test section will differ. The basics are the same, but, because I used this tunnel to test fog harvester prototypes I had to make an opening in the bottom for the drainage of the captured water and I added hooks to suspend the prototypes with.

I chose to make the test section out of plywood and make a window with plexiglass so I could observe what was going on. I have also seen designs where the whole test section was made out of plexiglass.

Think about what would suit your application best. The following instructions are based on the test section that I built.

1.1) Saw your plywood boards to size. Four boards of 60cm x 30cm in total. In two of them make openings, one for the drainage of water, the other one for the plexiglass window. Make sure to make the opening before putting them together, it is easier. Saw your beams to size. Also already add the hook screws on the place where you want to suspend your prototypes. It is a bit of hassle to put them in when your test section is already put together.

I made sure the prototypes could be suspended at 1/3 of the test section because then there is 2/3 of the test section left for the wake to develop.

1.2) Later I made the drainage area underneath the prototypes that I was testing larger. I did this by adding a slanted plated on the bottom of the test section. The 3D print for that drain can be found here: https://www.thingiverse.com/thing:3004841 (https://www.thingiverse.com/thing:3004841) If you don't have a 3D printer I am sure you can make something out of leftover plexiglass or a plate of plywood.

1.3) Because I wanted to measure the wind speed in my wind tunnel, I added a hole at the beginning of the test section. The beam of a 3 cup anemometer would fit through the hole and I was able to determine the wind speed inside the tunnel. (See picture)

2) Assembly the four boards with the beams in the same way as you did for the other sections.

3) Make the section water resistant with some sort of wood seal or dye and let it dry overnight. Add an extra layer for security if you have the time.
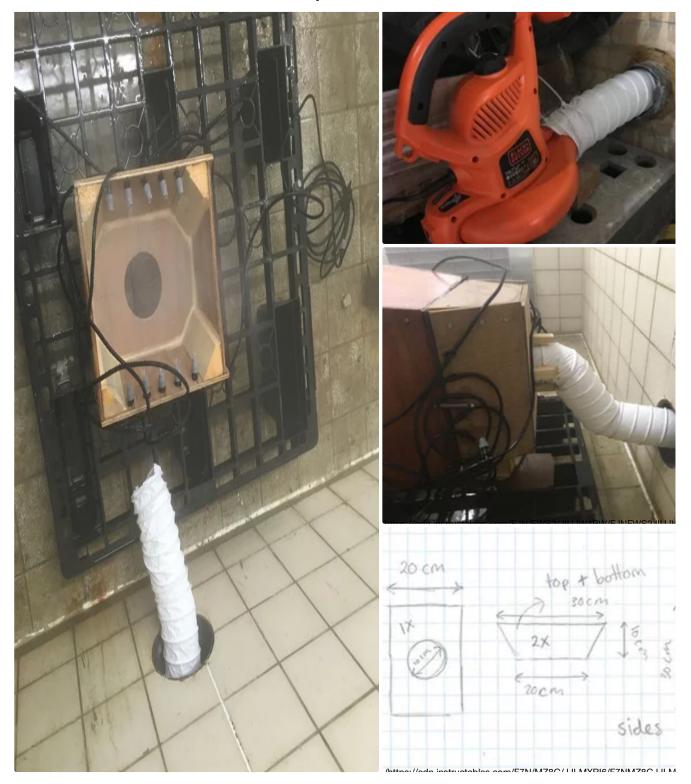
4) Add the plexiglass to create a window in your test section. I added the plexiglass on the inside of the test section and secured it with screws. I made sure the plexiglass would cover exactly one whole side of the test section so the side would still be one smooth side and the airstream wouldn't be interrupted.

5) At the edge that will be connected to the contraction cone, add the screws for hooking the springs and the airstrip.

Add Tip   Ask Question   Comment   Download

Step 5: Inlet

Just as with the test section, your inlet might differ from mine depending on what you have available and the purpose of your setup. I was working in a climate room and had to bring in the wind through a hole in the wall with a diameter of 12cm, the leaf blower was perfect for that. I added the mist at the inlet too.

Think about what would suit your application best. The following instructions are based on the inlet that worked best for my application.

1) Saw plywood and beams to size, add the hole where the tubing of the airstream will go through. The tube that I used had a diameter of 12cm, by making the diameter of the hole in the inlet a bit smaller the tube will jam.

2) Add holes in the side boards for the nozzles of the garden mist system to go through. The diameter of the holes will depend on the nozzles that you are using.

3) Assemble the boards with the beams in a similar way as with the previous sections.

4) Make the section water resistant with some sort of wood seal or dye and let it dry overnight. Add an extra layer for security if you have the time.

5) At the edge that will be connected to the diffuser, add the screws for hooking the springs and the airstrip.

5) Add the nozzles to the inlet. I was able to suspend the mist-making nozzles in the inlet by taking the nozzle part of the tubing, placing the tubing through the holes you made earlier and placing the nozzle back on the tube. (See picture)

6) Add the tubing for the airstream. As you can see in the picture, I added 4 small wooden blocks on the outside of the inlet around the tubing. I did this to make sure the airstream would enter the inlet parallel to the floor and not slightly up or down disturbing the air stream.

Add Tip   Ask Question   Comment   Download

Step 6: Assembly and Operation

With all the section built, made water resistant, screws for the springs, and airstrips in place it is time for to assemble them all.

1) Place all components end-to-end in the place where you are going to use the device. Be sure you can attach the hose for the mist nozzles to a tap close by. You will notice that all parts are not the same height and you will need to lift some parts. You can construct nice stands. Or make it easy for yourself and place some scrap pieces of wood underneath. For me, that worked fine.

2) One by one, connect the sections by their connecting screws, using the springs and make sure the inside of the tunnel is as smooth as possible.

3) You might notice that the transitions between the boards and beams aren't that smooth and the connections aren't too good either. Therefore, each time I added a new part I smoothed the corners and connections with duct tape. It is an easy and quick solution to ensure a smooth airflow inside your tunnel. Beware! Don't go cheap on your tape, choose a high-quality brand that can resist the water.
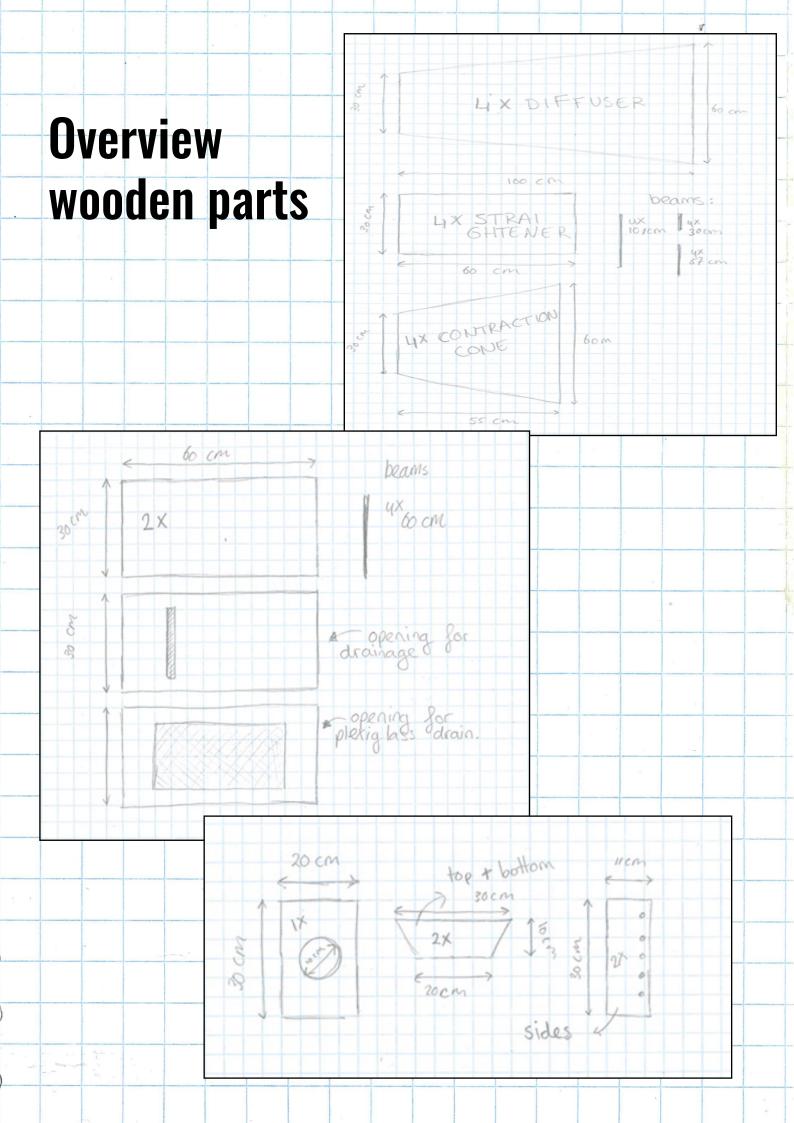
4) Connect the nozzle system to the tap, plug in the leafblower and start testing!

5) Enjoy!

Add Tip   Ask Question   Comment   Download

Share

Did you make this project? Share it with us!

I Made It!

Overview wooden parts

4 X DIFFUSER — 30 cm, 60 cm, 100 cm

4 X STRAIGHTENER — 30 cm, 60 cm

beams:
- 4x 10 cm
- 4x 30 cm
- 4x 57 cm

4 X CONTRACTION CONE — 30 cm, 60 cm, 55 cm

60 cm, 30 cm, 30 cm

2 X

beams
- 4x 60 cm

← opening for drainage

← opening for plexiglass drain.

20 cm, 30 cm — **1X** (10 cm)

top + bottom — **2X** — 30 cm, 20 cm, 10 cm

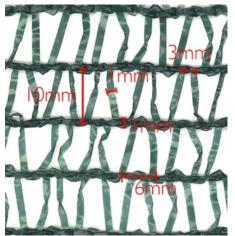sides — **2X** — 11 cm, 30 cm

5. Prototyping

This chapter gives an overview of all the prototypes that were tested during this study in a chronological order. The focus is on the materials that were used and how they were made. Experimental results are discussed in the following chapter. tags: #rapid prototyping #shade net #3D printing
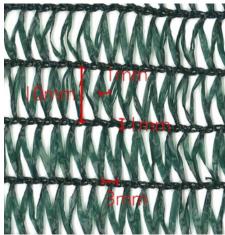
AT THE START OF THIS RESEARCH I WANTED TO FOCUS ON MATERIALS THAT ARE SUITABLE FOR FOG HARVESTING BUT CHEAP AND GLOBALLY AVAILABLE. I DECIDED TO USE SHADE NETS. THIS MATERIAL IS NORMALLY USED IN GREENHOUSES AND HAS BEEN PROVEN TO WORK FOR FOG HARVESTING PROJECTS. AT ALIBABA.COM THE BULK PRICES VARY FROM $0.10 TO $1.00 PER SQUARED METER.

I GOT MY HANDS ON SIX DIFFERENT SHADE NETS WITH VARYING SHADE COEFFICIENTS (SC), THE RATIO OF OCCLUDED AREA TO THE TOTAL NET AREA, AND STARTED WORKING WITH THEM TO MAKE THE FIRST PROTOTYPES.
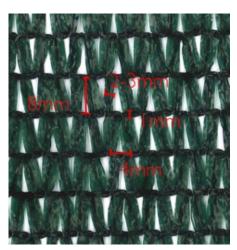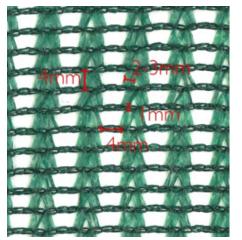
SHADE NETS

SC: 44.6%
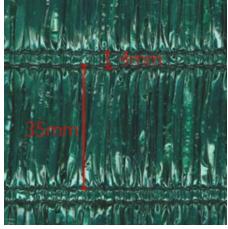Raschel knit
HDPE Plastic

SC: 69.9%
Raschel knit
HDPE Plastic

SC: 91.4%
Raschel knit
HDPE Plastic

SC: 71.2%
Raschel knit
HDPE Plastic

SC: 99.9%
Densley packed filaments
HDPE Plastic

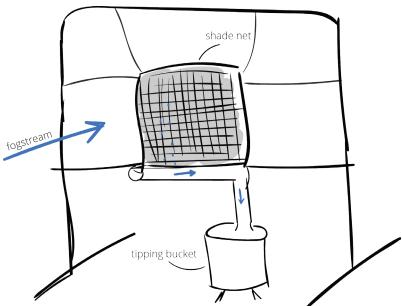SC: varies with suspension
here ±20%
HDPE Plastic

INTERESTING RESEARCH ABOUT SHADE NETS FOR FOG HARVESTING:

RIVERA, J., & LOPEZ-GARCIA, D. (2015). MECHANICAL CHARACTERISTICS OF RASCHEL MESH AND THEIR APPLICATION TO THE DESIGN OF LARGE FOG COLLECTORS. ATMOSPHERIC RESEARCH (VOL. 151). HTTPS://DOI.ORG/10.1016/J.ATMOSRES.2014.06.011

SHANYENGANA, E. S., SANDERSON, R. D., SEELY, M. K., & SCHEMENAUER, R. S. (N.D.). TESTING GREENHOUSE SHADE NETS IN COLLECTION OF FOG FOR WATER SUPPLY.

3.1 PROOF OF CONCEPT

A SIMPLE FOG CATCHER WAS BUILT INSIDE THE CLIMATE ROOM TO TEST IF THE MESHES WOULD ACTUALLY CAPTURE AND DRAIN FOG DROPLETS. THE FOG CATCHER FRAME WAS MADE OUT OF STEEL SCAFFOLDING PIPES, AND 30CM X 30CM PIECES OF SHADE NET WERE SUSPENDED IN THE FRAME. THE FRAME WAS PLACED IN FRONT OF ONE OF THE MIST NOZZLES PRESENT IN THE CLIMATE ROOM. A HALF-OPEN DRAIN WAS PLACED UNDERNEATH THE NET TO LEAD THE CAPTURED WATER TO A RAIN GAUGE TIPPING BUCKET.

Sketch of proof of concept fog catcher

Left) The simple fog catcher placed inside the climate room. Since it's intended purpose was just a proof concept it was built with material I still had, the scaffolding was left over from a previous project, I found the bamboo in the hallway of my student house, and everything is tied together with tie wraps and rope. Right) Drainage pipe ending at the tipping bucket.

3.2 PROTOTYPE N0.1

THE FIRST PROTOTYPES THAT WARE MADE FOR THE EXPERIMENTS INSIDE THE WIND TUNNEL CONSISTED OF THE NET SUSPENDED BETWEEN TWO WOODEN STICKS WITH SEWING THREAD. THE TOTAL SURFACE AREA WAS 10CM X 10CM. THE PROTOTYPES WERE SUSPENDED INSIDE THE TUNNEL USING THE SAME SEWING THREAD.

3.3 K'NEX PROTOTYPES

OF THE FIRST PROTOTYPES, ONLY TWO WERE MADE. BECAUSE THEY LACKED A FRAME, THEY FELT FEEBLE, AND THE MATERIAL DIDN'T LEND ITSELF TO CREATE DIFFERENT SHAPES WITH, SOMETHING THAT WAS ULTIMATELY THE GOAL. THEREFORE I SWITCH OVER TO MAKING PROTOTYPES WITH FRAMES MADE OUT OF K'NEX, THE PLASTIC CONSTRUCTION TOY. BECAUSE OF THE K'NEX DIMENSION THAT FRAMES HAD AN AREA OF 11CM X 11CM. AGAIN THE NET WAS SUSPENDED INSIDE THE FRAME USING SEWING THREAD. I SWITCH OVER TO SUSPENDING THE FRAMES WITH ELASTIC BANDS. BECAUSE THE SEWING THREAD WOULD SOMETIMES SNAP AND IT WAS VERY LABOR INTENSIVE TO SUSPEND THE NETS EACH TIME. BECAUSE ALL ELASTIC BANDS WERE ROUGHLY THE SAME SIZE, IT ALSO MADE SURE THAT THE NETS WERE SUSPENDED AT THE SAME HEIGHT IN THE TUNNEL EACH TIME.

3.4 HARP LIKE PROTOTYPES MADE OUT OF 99.9% SC FABRIC

INSPIRED BY THE RECENT WORK OF SHI ET AL. (2018)[4], A FIRST ATTEMPT WAS MADE TO CREATE HARP-LIKE FOG HARVESTERS. THE HARP-LIKE STRUCTURE IS SUPPOSED TO ENHANCE DRAINAGE AND REDUCE CLOGGING. THE PROTOTYPES WERE MADE BY USING THE FILAMENTS OF THE 99.9% SC FABRIC. THEY WERE HELD TOGETHER BY PIECES OF DUCT TAPE, WITH EXTRA STITCHING IN CASE THE TAPE WOULD LET LOOSE IN THE WET CLIMATE OF THE WIND TUNNEL.
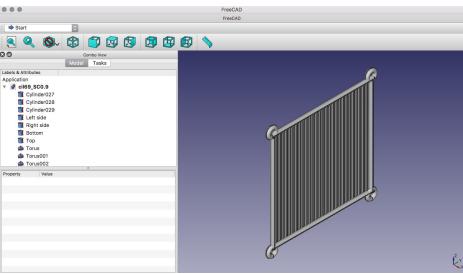

I WASN'T HAPPY WITH THE RESULT.

BECAUSE OF THE WAY THE FILAMENTS WERE INITIALLY TIED IN THE FABRIC, THE PLASTIC FILAMENTS WERE NOT NICE AND SMOOTH, AND IT WAS HARD TO SPACE THE FILAMENTS EQUALLY.
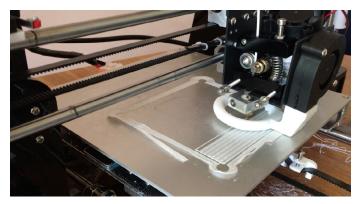
[4]Shi, W., Anderson, M. J., Tulko, J. B., Kennedy, B. S., & Boreyko, J. B. (2018). Fog Harvesting with Harps. https://doi.org/10.1021/acsami.7b17488

3.5 3D PRINTED HARP LIKE PROTOTYPES

THE FINAL PROTOTYPES THAT WERE USED DURING THIS PROJECT WERE MADE WITH AN ANET A8 3D PRINTER. USING THE OPENSOURCE SOFTWARE PROGRAM "FREECAD" A SET OF SIX DIFFERENT STRAIGHT FOG HARVESTER PROTOTYPES WITH VARYING SHADE COEFFICIENTS WERE MADE. TWO PROTOTYPES WITH A CURVED SHAPE WERE PRODUCED. THESE COULD EITHER BE USED CONCAVE OR CONVEX SHAPES, DEPENDING ON HOW THEY WERE FACING THE FOG STREAM.

EACH STRAIGHT PROTOTYPE NET CONSISTS OF A SQUARE FRAME OF CYLINDERS WITH A DIAMETER OF 4MM AND A TORUS WITH A DIAMETER OF 12MM AT EACH CORNER FOR SUSPENSION. THE FRAME WAS FILLED WITH FILAMENTS WITH A DIAMETER OF 1.3MM. EACH NET HAS A DIFFERENT NUMBER OF EQUALLY SPACED FILAMENTS TO VARY THE SHADE COEFFICIENT.

THE TWO CURVED NETS WERE PRINTED IN FIVE PARTS THAT WERE JOINED TOGETHER AFTER PRINTING. ONE NET HAD A CURVE EXTRUDING 20MM AND THE OTHER ONE 50MM.

Printscreen of FreeCAD software package, while working on a straight fog catcher prototype.

Anet A8 3D printing a prototype for the first time. This particular print started to go out of wack half way and never made it.

3D model of curved fog catcher prototype. The five seperate parts can be put together with a pins on some parts and holes in others.

IN TERMS OF GETTING THE PRINTS RIGHT YOU NEED A BIT OF UNDERSTANDING OF 3D PRINTING AND A GOOD DOSE OF PATIENCE. SOME THINGS TO TAKE INTO ACCOUNT ARE:

• MAKE SURE THE 3D DESIGN CAN BE PRINTED FLAT ON THE PRINTING BED. THE FILAMENTS ARE TOO THIN TO GO VERTICAL AND TOO LONG TO BE SUSPENDED IN THE AIR. THEREFORE, THE CURVED PROTOTYPES WERE PRINTED IN PARTS.

• THE PRINTED FILAMENT THICKNESS WILL DIFFER FROM THE DESIGN THICKNESS. THIS IS DEPENDED ON HOW CLOSE THE PRINT NOZZLE IS TO THE BED AND HOW MUCH THE PLASTIC STILL MELTS. SO AFTER THE FIRST GOOD PRINT, MEASURE THE THICKNESS AND DON'T CHANGE BED HEIGHT FOR THE FOLLOWING PRINTS.

• MAKE SURE ADHESION TO THE PRINTING BED IS GOOD. HAIR SPRAY AND GLUE STICKS DO WONDERS.

• BE PREPARED TO REDO PRINTS.

First five straight fog catcher prototypes with varying shade coefficients.

Curved prototype suspended inside the test section of the wind tunnel. At the bottom of the wind tunnel a 3D printed slanted plate is plate to ensure drainage of all water droplets shedding of the net.

CONCLUSION AND RECOMMENDATIONS

TESTING PROTOTYPES IN A WIND TUNNEL PROVIDED WITH A FOG STREAM IS A VALUABLE COMPLEMENT TO THE COMPUTATIONAL MODELS. IT CAN VALIDATE THE RESULTS FROM THE MODEL, AND YOU ARE ALSO ABLE TO OBSERVE THE EFFECTS THAT ARE NEGLECTED IN THE SIMULATIONS, SUCH AS DRAINAGE.

TESTING IN A WIND TUNNEL IS AN EXCELLENT INTERMEDIATE STEP BEFORE TESTING LARGE-SCALE FOG HARVESTERS IN THE FIELD. THE WIND TUNNEL IS RELATIVELY CHEAP TO CONSTRUCT, AND BECAUSE OF THE SMALL SCALE, THE PROTOTYPES ARE EASY TO PRODUCE. THIS GIVES YOU THE ABILITY TO TEST MANY DIFFERENT DESIGNS WHILE NOT BEING CONSTRAINT BY THE AVAILABILITY OF RESOURCES AND THE CLIMATE.

3D PRINTING IS A HELPFUL TOOL TO USE BECAUSE IT GIVES YOU FULL CONTROL OVER ALL VARIABLES OF THE DESIGN GEOMETRY. THIS GIVES YOU THE OPPORTUNITY TO SINGLE OUT ONE DESIGN PARAMETER AND ASSESS ITS INFLUENCE ON THE AMOUNT OF FOG WATER YOU COLLECT.

3D PRINTING FILES ARE AVAILABLE AT:

HTTPS://WWW.THINGIVERSE.COM/THING:3003416 (STRAIGHT)

HTTPS://WWW.THINGIVERSE.COM/THING:3003424 (CURVED)

6. Lab logbook

This chapter elaborates on the lab experiments and discusses some of the experimental results that were gathered during this study. Most of which are not so relevant for the academic paper and are therefore published here.

tags: #lab plan #procedure #results #discussion

AIM

The aim of the experiments was to gather experimental data to validate the CFD analysis done earlier in Ansys FLUENT. In particular, analyse the effect of the shade coefficient of the net on the total fog water collection rate.

The simulations showed, and theoretical analysis also indicates[5], water yield increases as shade coefficient increases until a maximum is reached around 50%-60%, after which yield decreases. According to the simulations and theory, water yield for a completely closed mesh is 0%, as all the water will go around the mesh following the air flow.

Later experiments were conducted to assess the influence of shape on the fog water collection rate, this is extensively elaborated in the academic paper accompanied to this document.

METHODS

We tested nets with different shade coefficients (SC) in a wind tunnel placed inside a climate chamber. Two versions of the wind tunnel were used, the first version is elaborated in chapter 2 of this document, the second version is explained in the paper. Details on the nets that were tested are given in chapter 3.

Water coming off the nets is captured via a drain hanging underneath the wind tunnel. The drain is connected to a ONSET tipping bucket rain gauge. Each tip is 3.9mL (based on lab calibration). The tipping bucket is covered for the remainder to avoid water from the humid climate chamber from entering.

Each experiment lasted 20 minutes, as this is long enough to achieve steady state. Nothing was dried in between each test but the first tip of a new test was disregarded during data analysis. (Water could still be presented in the tipping bucket at the start, net still has to saturate before drainage starts, etc.).

[5]Rivera, J. D. D. (2011). Aerodynamic collection efficiency of fog water collectors. Atmospheric Research, 102(3), 335–342. https://doi.org/10.1016/j.atmosres.2011.08.005

DESIGN OF EXPERIMENTS

Dependent variable: water yield

Independent variables: wind speed, shade coefficient of net and drainage direction

The nets with a shade coefficient of 20.8% and 99.9% were tested once per experimental round since there is no particular drainage direction. The other nets were tested twice, once for each drainage direction. (Due to the weave or knit of the mesh the drainages can be affected significantly, changing the water yield).

The wind speed was kept constant during the experiments.

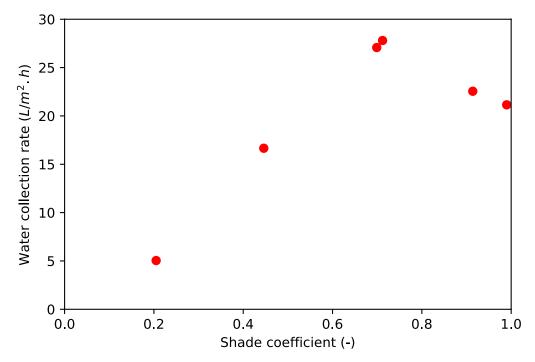Water collection rate was based on the time between each tip of the tipping bucket.

PROCEDURE

Start
*   Position tunnel at right position
*   Launch rain gauge
*   Check status
*   Place rain gauge in climate chamber
*   Suspend net
*   *Turn on leaf blower if applicable (version 1.0)*
*   *Turn on tap for the nozzles if applicable (version 1.0)*

Repeat
*   Suspend new net
*   Check if it is in the middle
*   Leave the room and shut door properly
*   Note down start time, type of mesh and wind speed
*   Start timer for 20 minutes
*   Note down end time after 20 minutes
*   Come back and 'soap' window and camera lens for
        clarity of filming
*   Film drainage process
*   Repeat

End
*   *Turn of leafblower if applicable (version 1.0)*
*   Divert water from coming into setup by turning
        water off (version 1.0) or moving the setup
        away from the nozzle (version 2.0)
*   Read out data from rain gauge
*   Charge camera

RESULTS AND DISCUSSION

PROOF OF CONCEPT

We tested six shade nets in a simple fog catcher set up (see chapter 4).

The results from this test are presented below. These results gave us the confidence that the net material is suitable for catching water droplets out of the fog stream. These results show that there is indeed an increase in water yield up to a specific shade coefficient, after which the yield decreases again, like the analytical model and CFD simulations predicted. These results gave us the confidence to proceed with building the wind tunnel and use the shade nets as harvesting material.

As the graph on the left shows, the shade net with an SC of 99.9% still captures water, although according to the theory this net should not capture any water. Theoreticall the airstream would carry all suspended droplets around the net. The fact that the nets does capture water could be due to the turbulence present in the fog stream at this distance from the nozzle.

Fog water collection rates tested for 20 minutes for six different shade nets in a crude fog collector set up. The performance of the nets increases as SC becomes larger, and reaches a maximum around 70%.
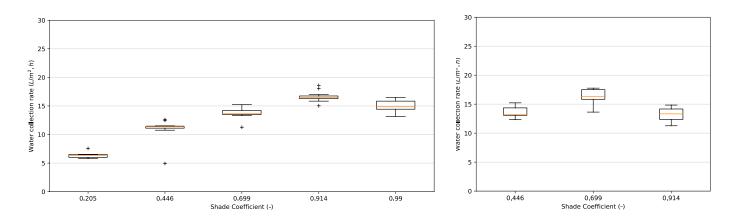
WIND TUNNEL VERSION 1.0

Tested five of the shade nets in the first version of the wind tunnel (see Chapter 4).

The results show an increase in water yield when the SC becomes larger. The analytical and CFD model predict a decrease in water yield after a shade coefficient of about 60% because the porosity becomes too small. In the results of the first wind tunnel experiments, we do not observe this drop.

We assumed that this was caused by the relatively large droplet diameter the garden hose nozzle produces, the droplet diameter is estimated to be around 100 micrometers. Therefore we decided to switch to version 2.0, making use of the pressurized nozzle present in the climate room.

For the nets with SC 44.6% and 69.9%, water yield increases when the net is turned around, for the net with SC 9.14% water yield decreases.

Left) Fog water collection rates tested for 20 minutes of five different shade nets with varying shade coefficients. The performance increase up to a shade coefficient of 69.9%, after that it stagnates. Right) For three net the water collection rates was determined again, but now the nets were turned around over 90 degrees in order to vary the drainage direction.
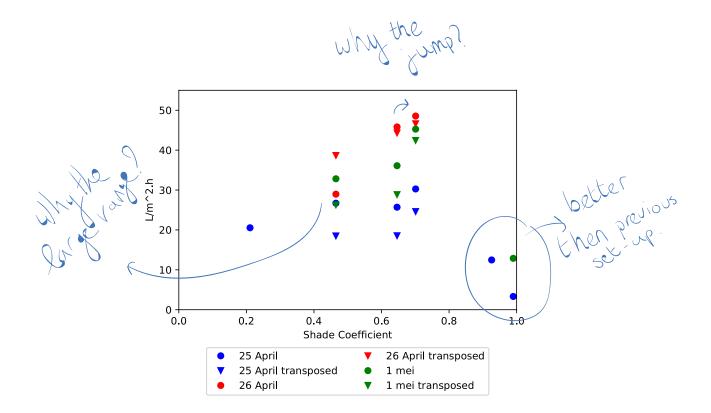
WIND TUNNEL VERSION 2.0

The second wind tunnel set up is discussed in detail in the academic paper. The most important thing to know is that this version made use of the pressurized nozzle available inside the climate room. Because of the pressure, the droplets are smaller. According to the manufacturer of the nozzle, the nozzle produces droplets in the range of 20 to 40 micrometers. Larger than the concentration peak of 10 micrometers found at fog sites, but covering part of the range of diameters found[6].

We tested six different shade nets, three of them in two directions (referred to as transposed). These three nets were also tested over three experiment runs. The results are presented in the graph on the next page.

The graph shows significant differences in water yield amongst the three experimental runs and differences when drainage direction is changed. On the first issue, after the experiments on day one, I would move the wind tunnel away from the nozzle so it wouldn't get to wet while I wasn't using it. Mold had already started to grow on the outside. The next time I would do an experimental run I would try to place the tunnel at the exact position based on pictures that I made. But the change in position might explain the differences amongst runs. Another important aspect that also explains the difference amongst the drainage directions is the clogging of the net. Because of the knit of the nets, one direction drains better than the other.

This also means that the drainage among the nets differs, explaining the water yield difference between the net with SC 69.9% and with SC 71.2%.

 [6]Schemenauer, R. S., & Joe, P. I. (1989). The Collection Efficiency of a Massive Fog Collector, 24, 53–69.

Figure shows scatter plot with x-axis "Shade Coefficient" (0.0 to 1.0) and y-axis "L/m^2.h" (0 to 50). Handwritten annotations read "Why the jump?", "Why the large range?", and "better then previous set-up."

Legend:
- 25 April (blue circle)
- 25 April transposed (blue triangle)
- 26 April (red circle)
- 26 April transposed (red triangle)
- 1 mei (green circle)
- 1 mei transposed (green triangle)

We started doing all these experiments with the aim to analyse the effect of the shade coefficient of the net on the total fog water collection rate. However, we noticed that changing from one shade net to another, more parameters would change besides the shade coefficient, because of the difference in knitting. While we didn't quite know the importance of the knitting, and it was also not an objective of this project to figure that out. It made it hard to draw conclusions from the results about the influence of shade coefficients, and we decided to change to harp-like 3D printed samples, such that the effects of drainage and clogging would be minimized.

The results of the experiments with the harp-like 3D printed samples are extensively discussed in the paper.